

Light Curves of Dwarf Plutonian Planets and other Large Kuiper Belt Objects: Their Rotations, Phase Functions and Absolute Magnitudes

Scott S. Sheppard

*Department of Terrestrial Magnetism, Carnegie Institution of Washington,
5241 Broad Branch Rd. NW, Washington, DC 20015
sheppard@dtm.ciw.edu*

ABSTRACT

I report new time-resolved light curves and determine the rotations and phase functions of several large Kuiper Belt objects, which includes the dwarf planet Eris (2003 UB₃₁₃). Three of the new sample of ten Trans-Neptunian objects display obvious short-term periodic light curves. (120348) 2004 TY₃₆₄ shows a light curve which if double-peaked has a period of 11.70 ± 0.01 hours and a peak-to-peak amplitude of 0.22 ± 0.02 magnitudes. (84922) 2003 VS₂ has a well defined double-peaked light curve of 7.41 ± 0.02 hours with a 0.21 ± 0.02 magnitude range. (126154) 2001 YH₁₄₀ shows variability of 0.21 ± 0.04 magnitudes with a possible 13.25 ± 0.2 hour single-peaked period. The seven new KBOs in the sample which show no discernible variations within the uncertainties on short rotational time scales are 2001 UQ₁₈, (55565) 2002 AW₁₉₇, (119979) 2002 WC₁₉, (120132) 2003 FY₁₂₈, (136108) Eris 2003 UB₃₁₃, (90482) Orcus 2004 DW, and (90568) 2004 GV₉. Four of the ten newly sampled Kuiper Belt objects were observed over a significant range of phase angles to determine their phase functions and absolute magnitudes. The three medium to large sized Kuiper Belt objects 2004 TY₃₆₄, Orcus and 2004 GV₉ show fairly steep linear phase curves (~ 0.18 to 0.26 mags per degree) between phase angles of 0.1 and 1.5 degrees. This is consistent with previous measurements obtained for moderately sized Kuiper Belt objects. The extremely large dwarf planet Eris (2003 UB₃₁₃) shows a shallower phase curve (0.09 ± 0.03 mags per degree) which is more similar to the other known dwarf planet Pluto. It appears the surface properties of the largest dwarf planets in the Kuiper Belt maybe different than the smaller Kuiper Belt objects. This may have to do with the larger objects ability to hold more volatile ices as well as sustain atmospheres. Finally, it is found that the absolute magnitudes obtained using the phase slopes found for individual objects are several tenths of magnitudes different than that given by the Minor Planet Center.

Subject headings: Kuiper Belt — Oort Cloud — minor planets, asteroids — solar system: general — planets and satellites: individual (2001 UQ₁₈, (126154) 2001 YH₁₄₀, (55565) 2002 AW₁₉₇, (119979) 2002 WC₁₉, (120132) 2003 FY₁₂₈, (136199) Eris 2003 UB₃₁₃, (84922) 2003 VS₂, (90482) Orcus 2004 DW, (90568) 2004 GV₉, and (120348) 2004 TY₃₆₄)

1. Introduction

To date only about 1% of the Trans-Neptunian objects (TNOs) are known of the nearly one hundred thousand expected larger than about 50 km in radius just beyond Neptune’s orbit (Trujillo et al. 2001). The majority of the largest Kuiper Belt objects (KBOs) now being called dwarf Plutonian planets (radii > 400 km) have only recently been discovered in the last few years (Brown et al. 2005). The large self gravity of the dwarf planets will allow them to be near Hydrostatic equilibrium, have possible tenuous atmospheres, retain extremely volatile ices such as Methane and are likely to be differentiated. Thus the surfaces as well as the interior physical characteristics of the largest TNOs may be significantly different than the smaller TNOs.

The largest TNOs have not been observed to have any remarkable differences from the smaller TNOs in optical and near infrared broad band color measurements (Doressoundiram et al. 2005; Barucci et al. 2005). But near infrared spectra has shown that only the three largest TNOs (Pluto, Eris (2003 UB₃₁₃) and (136472) 2005 FY₉) have obvious Methane on their surfaces while slightly smaller objects are either spectrally featureless or have strong water ice signatures (Brown et al. 2005; Licandro et al. 2006). In addition to the Near infrared spectra differences, the albedos of the larger objects appear to be predominately higher than those for the smaller objects (Cruikshank et al. 2005; Bertoldi et al. 2006; Brown et al. 2006). A final indication that the larger objects are indeed different is that the shapes of the largest KBOs seem to signify they are more likely to be in hydrostatic equilibrium than that for the smaller KBOs (Sheppard and Jewitt 2002; Trilling and Bernstein 2006; Lacerda and Luu 2006).

The Kuiper Belt has been dynamically and collisionally altered throughout the age of the solar system. The largest KBOs should have rotations that have been little influenced since the sculpting of the primordial Kuiper Belt. This is not the case for the smaller KBOs where recent collisions and fragmentation processes will have highly modified their spins throughout the age of the solar system (Davis and Farinella 1997). The large volatile rich KBOs show significantly different median period and possible amplitude rotational differences when compared to the rocky large main belt asteroids which is expected because of

their differing compositions and collisional histories (Sheppard and Jewitt 2002; Lacerda and Luu 2006).

I have furthered the photometric monitoring of large KBOs (absolute magnitudes $H < 5.5$ or radii greater than about 100 km assuming moderate albedos) in order to determine their short term rotational and long term phase related light curves to better understand their rotations, shapes and possible surface characteristics. This is a continuation of previous works (Jewitt and Sheppard 2002; Sheppard and Jewitt 2002; Sheppard and Jewitt 2003; Sheppard and Jewitt 2004).

2. Observations

The data for this work were obtained at the Dupont 2.5 meter telescope at Las Campanas in Chile and the University of Hawaii 2.2 meter telescope atop Mauna Kea in Hawaii.

Observations at the Dupont 2.5 meter telescope were performed on the nights of February 14, 15 and 16, March 9 and 10, October 25, 26, and 27, November 28, 29, and 30 and December 1, 2005 UT. The instrument used was the Tek5 with a 2048×2048 pixel CCD with $24 \mu\text{m}$ pixels giving a scale of $0.''259 \text{ pixel}^{-1}$ at the f/7.5 Cassegrain focus for a field of view of about $8'.85 \times 8'.85$. Images were acquired through a Harris R-band filter while the telescope was autoguided on nearby bright stars at sidereal rates (Table 1). Seeing was generally good and ranged from $0.''6$ to $1.''5$ FWHM.

Observations at the University of Hawaii 2.2 meter telescope were obtained on the nights of December 19, 21, 23 and 24, 2003 UT and used the Tektronix 2048×2048 pixel CCD. The pixels were $24 \mu\text{m}$ in size giving $0.''219 \text{ pixel}^{-1}$ scale at the f/10 Cassegrain focus for a field of view of about $7'.5 \times 7'.5$. Images were obtained in the R-band filter based on the Johnson-Kron-Cousins system with the telescope auto-guiding at sidereal rates using nearby bright stars. Seeing was very good over the several nights ranging from $0.''6$ to $1.''2$ FWHM.

For all observations the images were first bias subtracted and then flat-fielded using the median of a set of dithered images of the twilight sky. The photometry for the KBOs was done in two ways in order to optimize the signal-to-noise ratio. First, aperture correction photometry was performed by using a small aperture on the KBOs ($0.''65$ to $1.''04$ in radius) and both the same small aperture and a large aperture ($2.''63$ to $3.''63$ in radius) on several nearby unsaturated bright field stars. The magnitude within the small aperture used for the KBOs was corrected by determining the correction from the small to the large aperture using the PSF of the field stars. Second, I performed photometry on the KBOs using the same field stars but only using the large aperture on the KBOs. The smaller apertures allow better

photometry for the fainter objects since it uses only the high signal-to-noise central pixels. The range of radii varies because the actual radii used depends on the seeing. The worse the seeing the larger the radius of the aperture needed in order to optimize the photometry. Both techniques found similar results, though as expected, the smaller aperture gives less scatter for the fainter objects while the larger aperture is superior for the brighter objects.

Photometric standard stars from Landolt (1992) were used for calibration. Each individual object was observed at all times in the same filter and with the same telescope setup. Relative photometric calibration from night to night was very stable since the same fields stars were observed. The few observations that were taken in mildly non-photometric conditions (i.e. thin cirrus) were easily calibrated to observations of the same field stars on the photometric nights. Thus, the data points on these mildly non-photometric nights are almost as good as the other data with perhaps a slightly larger error bar. The dominate source of error in the photometry comes from simple root N noise.

3. Light Curve Causes

The apparent magnitude or brightness of an atmospherless inert body in our solar system is mainly from reflected sunlight and can be calculated as

$$m_R = m_{\odot} - 2.5 \log [p_R r^2 \phi(\alpha) / (2.25 \times 10^{16} R^2 \Delta^2)] \quad (1)$$

in which r [km] is the radius of the KBO, R [AU] is the heliocentric distance, Δ [AU] is the geocentric distance, m_{\odot} is the apparent red magnitude of the sun (-27.1), m_R is the apparent red magnitude, p_R is the red geometric albedo, and $\phi(\alpha)$ is the phase function in which the phase angle $\alpha = 0$ deg at opposition and $\phi(0) = 1$.

The apparent magnitude of the TNO may vary for the main following reasons:

1) The geometry in which R , Δ and/or α changes for the TNO. Geometrical considerations at the distances of the TNOs are usually only noticeable over a few weeks or longer and thus are considered long-term variations. These are further discussed in section 5.

2) The TNOs albedo, p_R , may not be uniform on its surface causing the apparent magnitude to vary as the different albedo markings on the TNOs surface rotate in and out of our line of sight. Albedo or surface variations on an object usually cause less than a 30% difference from maximum to minimum brightness of an object. (134340) Pluto, because of its atmosphere (Spencer et al. 1997), has one of the highest known amplitudes from albedo variations (~ 0.3 magnitudes; Buie et al. 1997).

3) Shape variations or elongation of an object will cause the effective radius of an object

to our line of sight to change as the TNO rotates. A double peaked periodic light curve is expected to be seen in this case since the projected cross section would go between two minima (short axis) and two maxima (long axis) during one complete rotation of the TNO. Elongation from material strength is likely for small TNOs ($r < 100$ km) but for the larger TNOs observed in this paper no significant elongation is expected from material strength because their large self gravity.

A large TNO ($r > 100$ km) may be significantly elongated if it has a large amount of rotational angular momentum. An object will be near breakup if it has a rotation period near the critical rotation period (P_{crit}) at which centripetal acceleration equals gravitational acceleration towards the center of a rotating spherical object,

$$P_{crit} = \left(\frac{3\pi}{G\rho} \right)^{1/2} \quad (2)$$

where G is the gravitational constant and ρ is the density of the object. With $\rho = 10^3$ kg m⁻³ the critical period is about 3.3 hours. At periods just below the critical period the object will likely break apart. For objects with rotations significantly above the critical period the shapes will be bimodal Maclaurin spheroids which do not show any significant rotational light curves produced by shape (Jewitt and Sheppard 2002). For periods just above the critical period the equilibrium figures are triaxial ellipsoids which are elongated from the large centripetal force and usually show prominent rotational light curves (Weidenschilling 1981; Holsapple 2001; Jewitt and Sheppard 2002).

For an object that is triaxially elongated the peak-to-peak amplitude of the rotational light curve allows for the determination of the projection of the body shape into the plane of the sky by (Binzel et al. 1989)

$$\Delta m = 2.5 \log \left(\frac{a}{b} \right) - 1.25 \log \left(\frac{a^2 \cos^2 \theta + c^2 \sin^2 \theta}{b^2 \cos^2 \theta + c^2 \sin^2 \theta} \right) \quad (3)$$

where $a \geq b \geq c$ are the semiaxes with the object in rotation about the c axis, Δm is expressed in magnitudes, and θ is the angle at which the rotation (c) axis is inclined to the line of sight (an object with $\theta = 90$ deg. is viewed equatorially). The amplitudes of the light curves produced from rotational elongation can range up to about 0.9 magnitudes (Leone et al. 1984).

Assuming $\theta = 90$ degrees gives $a/b = 10^{0.4\Delta m}$. Thus the easily measured quantities of the rotation period and amplitude can be used to determine a minimum density for an object if it is assumed to be rotationally elongated and strengthless (i.e. the body's structure behaves like a fluid, Chandrasekhar 1969). The two best cases of this high angular momentum

elongation in the Kuiper Belt are (20000) Varuna (Jewitt and Sheppard 2002) and (136108) 2003 EL₆₁ (Rabinowitz et al. 2006).

4) Periodic light curves may be produced if a TNO is an eclipsing or contact binary. A double-peaked light curve would be expected with a possible characteristic notch shape near the minimum of the light curve. Because the two objects may be tidally elongated the light curves can range up to about 1.2 magnitudes (Leone et al. 1984). The best example of such an object in the Kuiper Belt is 2001 QG₂₉₈ (Sheppard and Jewitt 2004).

5) A non-periodic short-term light curve may occur from a complex rotational state, a recent collision, a binary with each component having a large light curve amplitude and a different rotation period or outgassing/cometary activity. These types of short term variability are expected to be extremely rare and none have yet been reliably detected in the Kuiper Belt (Sheppard and Jewitt 2003; Belskaya et al. 2006)

4. Light Curve Results and Analysis

The photometric measurements for the 10 newly observed KBOs are listed in Table 1, where the columns include the start time of each integration, the corresponding Julian date, and the magnitude. No correction for light travel time has been made. Results of the light curve analysis for all the KBOs newly observed are summarized in Table 2.

The phase dispersion minimization (PDM) method (Stellingwerf 1978) was used to search for periodicity in the individual light curves. In PDM, the metric is the so-called Theta parameter, which is essentially the variance of the unphased data divided by the variance of the data when phased by a given period. The best fit period should have a very small dispersion compared to the unphased data and thus $\Theta \ll 1$ indicates that a good fit has been found. In practice, a Theta less than 0.4 indicates a possible periodic signature.

4.1. (120348) 2004 TY₃₆₄

Through the PDM analysis I found a strong Theta minima for 2004 TY₃₆₄ near a period of $P = 5.85$ hours with weaker alias periods flanking this (Figure 1). Phasing the data to all possible periods in the PDM plot with $\Theta < 0.4$ found that only the single-peaked period near 5.85 hours and the double-peaked period near 11.70 hours fits all the data obtained from October, November and December 2005. Both periods have an equally low Theta parameter of about 0.15 and either could be the true rotation period (Figures 2 and 3). The peak-to-peak amplitude is 0.22 ± 0.02 magnitudes.

If 2004 TY₃₆₄ has a double-peaked period it may be elongated from its high angular momentum. If the TNO is assumed to be observed equator on then from Equation 3 the $a : b$ axis ratio is about 1.2. Following Jewitt and Sheppard (2002) I assume the TNO is a rotationally elongated strengthless rubble pile. Using the spin period of 11.7 hours, the 1.2 $a : b$ axis ratio found above and the Jacobi ellipsoid tables produced by Chandrasekhar (1969) I find the minimum density of 2004 TY₃₆₄ is about 290 kg m⁻³ with an $a : c$ axis ratio of about 1.9. This density is quite low which leads one to believe either the TNO is not being viewed equator on or the relatively long double-peaked period is not created from high angular momentum of the object.

4.2. (84922) 2003 VS₂

The KBO 2003 VS₂ has a very low Theta of less than 0.1 near 7.41 hours in the PDM plot (Figure 4). Phasing the December 2003 data to this period shows a well defined double-peaked period (Figure 5). The single peaked period for this result would be near 3.71 hours which was a possible period determined for this object by Ortiz et al. (2006). The 3.71 hour single-peaked period does not look as convincing (Figure 6) which confirms the PDM result that the single-peaked period has about three times more dispersion than the double-peaked period. This is likely because one of the peaks is taller in amplitude (~ 0.05 mags) and a little wider. The other single-peaked period of 4.39 hours (Figure 7) and the double-peaked period of 8.77 hours (Figure 8) mentioned by Ortiz et al. (2006) do not show a low Theta in the PDM and also do not look convincing when examining the phased data. The peak-to-peak amplitude is 0.21 ± 0.02 magnitudes, which is similar to that detected by Ortiz et al. (2006).

The fast rotation of 7.41 hours and double-peaked nature suggests that 2003 VS₂ may be elongated from its high angular momentum. Using Equation 3 and assuming the TNO is observed equator on the $a : b$ axis ratio is about 1.2. Using the spin period of 7.41 hours, the 1.2 $a : b$ axis ratio and the Jacobi ellipsoid tables produced by Chandrasekhar (1969) I find the minimum density of 2003 VS₂ is about 720 kg m⁻³ with an $a : c$ axis ratio of about 1.9. This result is similar to other TNO densities found through the Jacobian Ellipsoid assumption (Jewitt and Sheppard 2002; Sheppard and Jewitt 2002; Rabinowitz et al. 2006) as well as recent thermal results from the Spitzer space telescope (Stansberry et al. 2006).

4.3. (126154) 2001 YH₁₄₀

(126154) 2001 YH₁₄₀ shows variability of 0.21 ± 0.04 magnitudes. The PDM for this TNO shows possible periods near 8.5, 9.15, 10.25 and 13.25 hours though only the 13.25 hour period has a Theta less than 0.4 (Figure 9). Visibly examining the phased data finds only the 13.25 hour period is viable (Figure 10). This is consistent with the observation that one minimum and one maximum were shown on December 23, 2003 in about six and a half hours, which would give a single-peaked light curve of twice this time or about 13.25 hours. Ortiz et al. (2006) found this object to have a similar variability but with very limited data could not obtain a reliable period. Ortiz et al. did have one period of 12.99 hours which may be consistent with our result.

4.4. Flat Rotation Curves

Seven of the ten newly observed KBOs; 2001 UQ₁₈, (55565) 2002 AW₁₉₇, (119979) 2002 WC₁₉, (120132) 2003 FY₁₂₈, (136199) Eris 2003 UB₃₁₃, (90482) Orcus 2004 DW, and (90568) 2004 GV₉ showed no variability within the photometric uncertainties of the observations (Table 2; Figures 11 to 21). These KBOs thus either have extremely long rotational periods, are viewed nearly pole-on or most likely have small peak-to-peak rotational amplitudes. The upper limits for the objects short-term rotational variability as shown in Table 2 were determined through a monte carlo simulation. The monte carlo simulation determined the lowest possible amplitude that would be seen in the data from the time sampling and variance of the photometry as well as the errors on the individual points.

Ortiz et al. (2006) reported a possible 0.04 ± 0.02 photometric range for (90482) Orcus 2004 DW and a period near 10 hours. I do not confirm this result here. Ortiz et al. (2006) also reported a marginal 0.08 ± 0.03 photometric range for (55565) 2002 AW₁₉₇ with no one clear best period. I can not confirm this result and find that for 2002 AW₁₉₇ the rotational variability appears significantly less than 0.08 magnitudes.

Some of the KBOs in this sample appear to have variability which is just below the threshold of the data detection and thus no significant period could be obtained with the current data. In particular 2001 UQ₁₈ appears to have a light curve with a significant amplitude above 0.1 magnitudes but the data is sparser for this object than most the others and thus no significant period is found. Followup observations will be required in order to determine if most of these flat light curve objects do have any significant short-term variability.

4.5. Comparisons with Size, Amplitude, Period, and MBAs

In Figures 22 and 23 are plotted the diameters of the largest TNOs and Main Belt Asteroids (MBAs) versus rotational amplitude and period, respectively. Most outliers on Figure 22 can easily be explained from the discussion in section 3. Varuna, 2003 EL₆₁ and the other unmarked TNOs with photometric ranges above about 0.4 magnitudes are all spinning faster than about 8 hours. They are thus likely hydrostatic equilibrium triaxial Jacobian ellipsoids which are elongated from their rotational angular momentum (Jewitt and Sheppard 2002; Sheppard and Jewitt 2002; Rabinowitz et al. 2006). 2001 QG₂₉₈'s large photometric range is probably because this object is a contact binary indicative of its longer period and notched shaped light curve (Sheppard and Jewitt 2004). Pluto's relatively large amplitude light curve is best explained through its active atmosphere (Spencer et al. 1997). Like the MBAs, the photometric amplitudes of the TNOs start to increase significantly at sizes less than about 300 km in diameter. The likely reason is this size range is where the objects are still large enough to be dominated by self-gravity and are not easily disrupted through collisions but can still have their angular momentum highly altered from the collisional process (Farinella et al. 1982; Davis and Farinella 1997). Thus this is the region most likely to be populated by high angular momentum triaxial Jacobian ellipsoids (Farinella et al. 1992).

From this work Eris (2003 UB₃₁₃) has one of the highest signal-to-noise time-resolved photometry measurements of any TNO searched for a rotational period. There is no obvious rotational light curve larger than about 0.01 magnitudes in our extensive data which indicates a very uniform surface, a rotation period of over a few days or a pole-on viewing geometry. Carraro et al. (2006) suggest a possible 0.05 magnitude variability for Eris between nights but this is not obvious in this data set. The similar inferred composition and size of Eris to Pluto suggests these objects should behave very similar (Brown et al. 2005, 2006). Since Pluto has a relatively substantial atmosphere at its current position of about 30 AU (Elliot et al. 2003; Sicardy et al. 2003) it is very likely that Eris has an active atmosphere when near its perihelion of 38 AU. At Eris' current distance of 97 AU its surface thermal temperature should be over 20 degrees colder than when at perihelion. Like Pluto, Eris' putative atmosphere near perihelion would likely be composed of N₂, CH₄ or CO which would mostly condense when near aphelion (Spencer et al. 1997; Hubbard 2003), effectively resurfacing the TNO every few hundred years. This is the most likely explanation as to why the surface of Eris appears so uniform. This may also be true for 2005 FY₉ which appears compositionally similar to Pluto (Licandro et al. 2006) and at 52 AU is about 15 degrees colder than Pluto.

Figure 23 shows that the median rotation period distribution for TNOs is about $9.5 \pm$

1 hours which is marginally larger than for similarly sized main belt asteroids (7.0 ± 1 hours)(Sheppard and Jewitt 2002; and Lacerda and Luu 2006). If confirmed, the likely reason for this difference are the collisional histories of each reservoir as well as the objects compositions.

5. Phase Curve Results

The phase function of an objects surface mostly depends on the albedo, texture and particle structure of the regolith. Four of the newly imaged TNOs (Eris 2003 UB₃₁₃, (120348) 2004 TY₃₆₄, Orcus 2004 DW, and (90568) 2004 GV₉) were viewed on two separate telescope observing runs occurring at significantly different phase angles (Figures 24 to 27). This allowed their linear phase functions,

$$\phi(\alpha) = 10^{-0.4\beta\alpha} \quad (4)$$

to be estimated where α is the phase angle in degrees and β is the linear phase coefficient in magnitudes per degree (Table 3). The phase angles for TNOs are always less than about 2 degrees as seen from the Earth. Most atmosphereless bodies show opposition effects at such small phase angles (Muinonen et al. 2002). The TNOs appear to have mostly linear phase curves between phase angles of about 2 and 0.1 degrees (Sheppard and Jewitt 2002,2003; Rabinowitz et al. 2007). For phase angles smaller than about 0.1 degrees TNOs may display an opposition spike (Hicks et al. 2005; Belskaya et al. 2006).

The moderate to large KBOs Orcus, 2004 TY₃₆₄, and 2004 GV₉ show steep linear R-band phase slopes (0.18 to 0.26 mags per degree) similar to previous measurements of similarly sized moderate to large TNOs (Sheppard and Jewitt 2002,2003; Rabinowitz et al. 2007). In contrast the extremely large dwarf planet Eris (2003 UB₃₁₃) has a shallower phase slope (0.09 mags per degree) more similar to Charon (~ 0.09 mags/deg; Buie et al. (1997)) and possibly Pluto (~ 0.03 mags/deg; Buratti et al. (2003)). Empirically lower phase coefficients between 0.5 and 2 degrees may correspond to bright icy objects whose surfaces have probably been recently resurfaced such as Triton, Pluto and Europa (Buie et al. 1997; Buratti et al. 2003; Rabinowitz et al. 2007). Thus Eris' low β is consistent with it having an icy surface that has recently been resurfaced.

In Figures 28 to 32 are plotted the linear phase coefficients found for several TNOs versus several different parameters (reduced magnitude, albedo, rotational photometric amplitude and $B - I$ broad band color). Table 4 shows the significance of any correlations. Based on only a few large objects it appears that the larger TNOs may have lower β values. This is true for the R-band and V-band data at the 97% confidence level but interestingly using

data from Rabinowitz et al. (2007) no correlation is seen in the I-band (Table 4). Thus further measurements are needed to determine if there is a significantly strong correlation between the size and phase function of TNOs. Further, it may be that the albedos are anti-correlated with β , but since we have such a small number of albedos known the statistics don't give a good confidence in this correlation. If confirmed with additional observations, these correlations may be an indication that larger TNOs surfaces are less susceptible to phase angle opposition effects at optical wavelengths. This could be because the larger TNOs have different surface properties from smaller TNOs due to active atmospheres, stronger self-gravity or different surface layers from possible differentiation.

5.1. Absolute Magnitudes

From the linear phase coefficient the reduced magnitude, $m_R(1, 1, 0) = m_R - 5\log(R\Delta)$ or absolute magnitude H (Bowell et al. 1989), which is the magnitude of an object if it could be observed at heliocentric and geocentric distances of 1 AU and a phase angle of 0 degrees, can be estimated (see Sheppard and Jewitt 2002 for further details). The results for $m_R(1, 1, 0)$ and H are found to be consistent to within a couple hundredths of a magnitude (Table 3 and Figures 24 to 27). It is found that the R-band empirically determined absolute magnitudes of individual TNOs appears to be several tenths of a magnitude different than what is given by the Minor Planet Center (Table 3). This is likely because the MPC assumes a generic phase function and color for all TNOs while these two physical properties appear to be significantly different for individual KBOs (Jewitt and Luu 1998). The work by Romanishin and Tegler (2005) attempts to determine various absolute magnitudes of TNOs by using main belt asteroid type phase curves which are not appropriate for TNOs (Sheppard and Jewitt 2002).

6. Summary

Ten large trans-Neptunian objects were observed in the R-band to determine photometric variability on times scales of hours, days and months.

1) Three of the TNOs show obvious short-term photometric variability which is taken to correspond to their rotational states.

- (120348) 2004 TY₃₆₄ shows a double-peaked period of 11.7 hours and if single-peaked is 5.85 hours. The peak-to-peak amplitude of the light curve is 0.22 ± 0.02 mags.

- (84922) 2003 VS₂ has a well defined double-peaked period of 7.41 hours with a peak-to-peak amplitude of 0.21 ± 0.02 mags. If the light curve is from elongation than 2003 VS₂'s a/b axis ratio is at least 1.2 and the a/c axis ratio is about 1.9. Assuming 2003 VS₂ is elongated from its high angular momentum and is a strengthless rubble pile it would have a minimum density of about 720 kg m^{-3} .
- (126154) 2001 YH₁₄₀ has a single-peaked period of about 13.25 hours with a photometric range of 0.21 ± 0.04 mags.

2) Seven of the TNOs show no short-term photometric variability within the measurement uncertainties.

- Photometric measurements of the large TNOs (90482) Orcus and (55565) 2002 AW₁₉₇ showed no variability within or uncertainties. Thus these measurements do not confirm possible small photometric variability found for these TNOs by Ortiz et al. (2006).
- No short-term photometric variability was found for (136199) Eris 2003 UB₃₁₃ to about the 0.01 magnitude level. This high signal to noise photometry suggests Eris is nearly spherical with a very uniform surface. Such a nearly uniform surface may be explained by an atmosphere which is frozen onto the surface of Eris when near aphelion. The atmosphere, like Pluto's, may become active when near perihelion effectively resurfacing Eris every few hundred years. The Methane rich TNO 2005 FY₉ may also be in a similar situation.

3) Four of the TNOs were observed over significantly different phase angles allowing their long term photometric variability to be measured between phase angles of 0.1 and 1.5 degrees.

- TNOs Orcus, 2004 TY₃₆₄ and 2004 GV₉ show steep linear R-band phase slopes between 0.18 and 0.26 mags/degree.
- Eris 2003 UB₃₁₃ shows a shallower R-band phase slope of 0.09 mags/degree. This is consistent with Eris having a high albedo, icy surface which may have recently been resurfaced.
- At the 97% confidence level the largest TNOs have shallower R-band linear phase slopes compared to smaller TNOs. The largest TNOs surfaces may differ from the smaller TNOs because of their more volatile ice inventory, increased self-gravity, active atmospheres, differentiation process or collisional history.

3) The absolute magnitudes determined for several TNOs through measuring their phase curves show a difference of several tenths of a magnitude from the Minor Planet Center values.

- The values found for the reduced magnitude, $m_R(1, 1, 0)$, and absolute magnitude, H , are similar to within a few hundredths of a magnitude for most TNOs.

Acknowledgments

Support for this work was provided by NASA through Hubble Fellowship grant # HF-01178.01-A awarded by the Space Telescope Science Institute, which is operated by the Association of Universities for Research in Astronomy, Inc., for NASA, under contract NAS 5-26555.

REFERENCES

- Barucci, M., Belskaya, I., Fulchignoni, M. & Birlan, M. 2005, *AJ*, 130, 1291
- Belskaya, I., Ortiz, J., Rousselot, P., Ivanova, V., Borisov, G., Shevchenko, V. & Peixinho, N. 2006, *Icarus*, 184, 277
- Bertoldi, F., Altenhoff, W., Weiss, A., Menten, K. & Thum, C. 2006, *Nature*, 439, 563
- Binzel, R., Farinella, P., Zappala V., & Cellino, A. 1989, in *Asteroids II*, ed. R. Binzel, T. Gehrels, and M. Matthews (Tucson: Univ. of Arizona Press), 416
- Bowell, E., Hapke, B., Domingue, D., Lumme, K., Peltoniemi, J., & Harris, A. 1989, in *Asteroids II*, ed. R. Binzel, T. Gehrels, and M. Matthews (Tucson: Univ. of Arizona Press), 524
- Brown, M., Trujillo, C. & Rabinowitz, D. 2005, *ApJ*, 635, L97
- Brown, M., Schaller, E., Roe, H., Rabinowitz, D., & Trujillo, C. 2006, *ApJ*, 643, L61
- Buie, M., Tholen, D. & Wasserman, L. 1997, *Icarus*, 125, 233
- Buratti, B., Hillier, J., Heinze, A., Hicks, M., Tryka, K., Mosher, J., Ward, J., Garske, M., Young, J. and Atienza-Rosel, J. 2003, *Icarus*, 162, 171
- Carraro, G., Maris, M., Bertin, D. and Parisi, M. 2006, *AA*, 460, L39
- Chandrasekhar, S. 1969, *Ellipsoidal Figures of Equilibrium*. Yale Univ. Press, New Haven, Conn.

- Cruikshank, D., Stansberry, J., Emery, J., Fernandez, Y., Werner, M., Trilling, D. & Rieke, G. 2005, *ApJ*, 624, 53
- Cruikshank, D., Barucci, M., Emery, J., Fernandez, Y., Grundy, W., Noll, K. and Stansberry, J. 2006, in *Protostars and Planets V*, ed. B. Reipurth, D. Jewitt, and K. Keil (Tucson: Univ. of Arizona Press), in press
- Davis, D. and Farinella, P. 1997, *Icarus*, 125, 50
- de Bergh, C., Delsanti, A., Tozzi, G., Dotto, E., Doressoundiram, A. and Barucci, M. 2005, *AA*, 437, 1115
- Doressoundiram, A., Peixinho, N., Doucet, C., Mousis, O., Barucci, M., Petit, J. and Veillet, C. 2005, *Icarus*, 174, 90
- Elliot, J., Ates, A., Babcock, B. et al. 2003, *Nature*, 424, 165
- Farinella, P. and Paolicchi, P. 1982, *Icarus*, 52, 409
- Farinella, P., Davis, D., Paolicchi, P., Cellino, A. and Zappala, V. 1992, *AA*, 253, 604
- Hicks, M., Simonelli, D. and Buratti, B. 2005, *Icarus*, 176, 492
- Holsapple, K. 2001, *Icarus*, 154, 432
- Hubbard, W. 2003, *Nature*, 424, 137
- Jewitt, D. & Luu, J. 1998, *AJ*, 115, 1667
- Jewitt, D. & Sheppard, S. 2002, *AJ*, 123, 2110
- Lacerda, P. & Luu, J. 2006, *AJ*, 131, 2314
- Landolt, A. 1992, *AJ*, 104, 340
- Leone, G., Farinella, P., Paolicchi, P. & Zappala, V. 1984, *A&A*, 140, 265
- Licandro, J., Pinilla-Alonso, N., Pedani, M., Oliva, E., Tozzi, G. and Grundy, W. 2006, *A&A*, 445, L35
- Muironen, K., Piironen, J., Shkuratov, Y., Ovcharenko, A. and Clark, B. 2002, in *Asteroids III*, ed. W. Bottke, A. Cellino, P. Paolicchi and R. Binzel (Tucson: Univ. of Arizona Press), 123
- Ortiz, J., Gutierrez, P., Santos-Sanz, P., Casanova, V. and Sota, A. 2006, *A&A*, 447, 1131
- Rabinowitz, D., Barkume, K., Brown, M. et al. 2006, *ApJ*, 639, 1238
- Rabinowitz, D., Schaefer, B. and Tourtellotte, S. 2007, *AJ*, 133, 26
- Romanishin, W. and Tegler, S. 2005, *Icarus*, 179, 523
- Sheppard, S. & Jewitt, D. 2002, *AJ*, 124, 1757

- Sheppard, S. & Jewitt, D. 2003, EM&P, 92, 207
- Sheppard, S. & Jewitt, D. 2004, AJ, 127, 3023
- Sicardy, B., Widemann, T., Lellouch, E. et al. 2003, Nature, 424, 168
- Spencer, J., Stansberry, J., Trafton, L., Young, E., Binzel, R. and Croft, S. 1997, in Pluto and Charon, ed. S. Stern and D. Tholen (Tucson: Univ. of Arizona Press), 435
- Stansberry, J., Grundy, W., Margot, J., Cruikshank, D., Emery, J., Rieke, G. and Trilling, D. 2006, ApJ, 643, 556
- Stellingwerf, R. 1978, ApJ, 224, 953
- Trilling, D. & Bernstein, G. 2006, AJ, 131, 1149
- Trujillo, C., Jewitt, D. & Luu, J. 2001, AJ, 122, 457
- Weidenschilling, S. 1981, Icarus, 46, 124

Table 1. Observations of Kuiper Belt Objects

Name	Image ^a	Airmass	Exp ^b (sec)	UT Date ^c yyyy mm dd.ddddd	Mag. ^d (m_R)	Err (m_R)
2001 UQ ₁₈	uq1223n3025	1.17	320	2003 12 23.22561	22.20	0.04
	uq1223n3026	1.15	320	2003 12 23.23060	22.30	0.04
	uq1223n3038	1.02	320	2003 12 23.28384	22.38	0.04
	uq1223n3039	1.01	320	2003 12 23.28882	22.56	0.04
	uq1223n3051	1.01	350	2003 12 23.34333	22.40	0.04
	uq1223n3052	1.01	350	2003 12 23.35123	22.48	0.04
	uq1223n3070	1.15	350	2003 12 23.41007	22.37	0.04
	uq1223n3071	1.17	350	2003 12 23.41540	22.28	0.04
	uq1224n4024	1.21	350	2003 12 24.21433	22.30	0.03
	uq1224n4025	1.19	350	2003 12 24.21969	22.15	0.03
	uq1224n4033	1.03	350	2003 12 24.27591	22.07	0.03
	uq1224n4034	1.02	350	2003 12 24.28125	22.04	0.03
	uq1224n4041	1.00	350	2003 12 24.31300	22.11	0.03
	uq1224n4042	1.00	350	2003 12 24.31834	22.14	0.03
	uq1224n4051	1.04	350	2003 12 24.36433	22.22	0.03
	uq1224n4052	1.05	350	2003 12 24.36967	22.18	0.03
	uq1224n4061	1.17	350	2003 12 24.41216	22.27	0.03
	uq1224n4062	1.20	350	2003 12 24.41750	22.22	0.03
	uq1224n4072	1.50	350	2003 12 24.46253	22.14	0.03
	uq1224n4073	1.56	350	2003 12 24.46781	22.09	0.03
(126154) 2001 YH ₁₄₀	yh1219n1073	1.10	300	2003 12 19.42900	20.85	0.02
	yh1219n1074	1.08	300	2003 12 19.43381	20.82	0.02
	yh1219n1084	1.01	300	2003 12 19.47450	20.81	0.02
	yh1219n1085	1.01	300	2003 12 19.47935	20.79	0.02
	yh1219n1092	1.00	300	2003 12 19.51172	20.77	0.02
	yh1219n1093	1.00	300	2003 12 19.51657	20.80	0.02
	yh1219n1112	1.06	300	2003 12 19.56332	20.86	0.02
	yh1219n1113	1.08	300	2003 12 19.56815	20.80	0.02
	yh1219n1116	1.15	350	2003 12 19.59215	20.81	0.02
	yh1219n1117	1.18	350	2003 12 19.59764	20.79	0.02

Table 1—Continued

Name	Image ^a	Airmass	Exp ^b (sec)	UT Date ^c yyyy mm dd.ddddd	Mag. ^d (m_R)	Err (m_R)
yh1219n1122		1.36	350	2003 12 19.63042	20.87	0.02
yh1219n1123		1.41	350	2003 12 19.63587	20.85	0.02
yh1219n1125		1.50	350	2003 12 19.64669	20.95	0.03
yh1221n2067		1.46	300	2003 12 21.35652	20.98	0.02
yh1221n2068		1.42	300	2003 12 21.36124	20.92	0.02
yh1223n3059		1.24	300	2003 12 23.38285	20.86	0.02
yh1223n3060		1.21	300	2003 12 23.38762	20.89	0.02
yh1223n3078		1.03	300	2003 12 23.44626	20.88	0.02
yh1223n3079		1.02	300	2003 12 23.45102	20.87	0.02
yh1223n3086		1.00	300	2003 12 23.48192	20.92	0.02
yh1223n3087		1.00	300	2003 12 23.48668	20.91	0.02
yh1223n3091		1.00	300	2003 12 23.51268	20.94	0.02
yh1223n3092		1.01	300	2003 12 23.51744	20.95	0.02
yh1223n3101		1.08	300	2003 12 23.55695	20.92	0.02
yh1223n3102		1.09	300	2003 12 23.56169	20.96	0.03
yh1223n3106		1.18	300	2003 12 23.58754	20.98	0.03
yh1223n3107		1.20	300	2003 12 23.59231	21.01	0.03
yh1223n3114		1.31	300	2003 12 23.61182	21.03	0.03
yh1223n3115		1.34	300	2003 12 23.61659	20.99	0.03
yh1223n3119		1.56	300	2003 12 23.64084	20.99	0.03
yh1224n4047		1.49	300	2003 12 24.34589	20.90	0.02
yh1224n4048		1.44	300	2003 12 24.35066	20.91	0.02
yh1224n4057		1.18	300	2003 12 24.39217	20.85	0.02
yh1224n4058		1.16	300	2003 12 24.39693	20.85	0.02
yh1224n4068		1.03	300	2003 12 24.44421	20.87	0.02
yh1224n4069		1.02	300	2003 12 24.44898	20.87	0.02
yh1224n4080		1.00	300	2003 12 24.49899	20.84	0.02
yh1224n4081		1.00	300	2003 12 24.50375	20.86	0.02
yh1224n4088		1.02	300	2003 12 24.52567	20.82	0.02
yh1224n4089		1.03	300	2003 12 24.53043	20.83	0.02

Table 1—Continued

Name		Image ^a	Airmass	Exp ^b (sec)	UT Date ^c yyyy mm dd.ddddd	Mag. ^d (m_R)	Err (m_R)
(55565)	2002 AW ₁₉₇	yh1224n4093	1.08	300	2003 12 24.55588	20.81	0.02
		yh1224n4094	1.09	300	2003 12 24.56065	20.82	0.02
		yh1224n4102	1.23	300	2003 12 24.59447	20.87	0.02
		yh1224n4103	1.25	300	2003 12 24.59926	20.82	0.02
		yh1224n4107	1.44	300	2003 12 24.62661	20.87	0.02
		aw1223n3088	1.09	220	2003 12 23.49223	19.89	0.01
		aw1223n3089	1.08	220	2003 12 23.49606	19.89	0.01
		aw1223n3093	1.03	220	2003 12 23.52320	19.87	0.01
		aw1223n3094	1.03	220	2003 12 23.52704	19.88	0.01
		aw1223n3103	1.02	220	2003 12 23.56663	19.89	0.01
		aw1223n3104	1.02	220	2003 12 23.57046	19.89	0.01
		aw1223n3108	1.05	220	2003 12 23.59807	19.89	0.01
		aw1223n3109	1.06	220	2003 12 23.60190	19.89	0.01
		aw1223n3116	1.11	220	2003 12 23.62171	19.87	0.01
		aw1223n3117	1.12	220	2003 12 23.62556	19.89	0.01
		aw1223n3122	1.26	220	2003 12 23.65822	19.87	0.01
		aw1223n3123	1.28	220	2003 12 23.66201	19.89	0.01
		aw1224n4066	1.34	220	2003 12 24.43521	19.87	0.01
		aw1224n4067	1.32	220	2003 12 24.43903	19.86	0.01
		aw1224n4078	1.09	220	2003 12 24.48975	19.89	0.01
		aw1224n4079	1.08	220	2003 12 24.49358	19.89	0.01
		aw1224n4086	1.04	220	2003 12 24.51683	19.86	0.01
		aw1224n4087	1.03	220	2003 12 24.52066	19.89	0.01
		aw1224n4091	1.01	220	2003 12 24.54768	19.90	0.01
		aw1224n4092	1.01	220	2003 12 24.55158	19.90	0.01
		aw1224n4100	1.04	220	2003 12 24.58659	19.86	0.01
		aw1224n4101	1.04	220	2003 12 24.59042	19.86	0.01
		aw1224n4105	1.10	220	2003 12 24.61789	19.86	0.01
		aw1224n4106	1.12	220	2003 12 24.62172	19.87	0.01
		aw1224n4111	1.25	220	2003 12 24.65382	19.86	0.01

Table 1—Continued

Name		Image ^a	Airmass	Exp ^b (sec)	UT Date ^c yyyy mm dd.ddddd	Mag. ^d (m_R)	Err (m_R)
(119979)	2002 WC ₁₉	aw1224n4112	1.27	220	2003 12 24.65766	19.87	0.01
		aw1224n4113	1.30	220	2003 12 24.66150	19.88	0.01
		aw1224n4114	1.32	220	2003 12 24.66534	19.88	0.01
		wc1219n1033	1.19	350	2003 12 19.27766	20.56	0.02
		wc1219n1045	1.05	300	2003 12 19.32341	20.61	0.02
		wc1219n1046	1.04	300	2003 12 19.32826	20.59	0.02
		wc1219n1057	1.00	300	2003 12 19.36042	20.60	0.02
		wc1219n1058	1.00	300	2003 12 19.36529	20.57	0.02
		wc1219n1066	1.01	300	2003 12 19.40263	20.56	0.02
		wc1219n1067	1.02	300	2003 12 19.40748	20.57	0.02
		wc1219n1077	1.11	300	2003 12 19.44804	20.61	0.02
		wc1219n1078	1.12	300	2003 12 19.45289	20.58	0.02
		wc1219n1088	1.33	300	2003 12 19.49419	20.59	0.02
		wc1219n1089	1.37	300	2003 12 19.49909	20.55	0.02
		wc1219n1094	1.58	300	2003 12 19.52222	20.57	0.02
		wc1219n1095	1.64	300	2003 12 19.52704	20.58	0.02
		wc1221n2026	1.64	300	2003 12 21.21505	20.56	0.02
		wc1221n2027	1.59	300	2003 12 21.21980	20.57	0.02
		wc1221n2042	1.26	300	2003 12 21.25881	20.55	0.02
		wc1221n2043	1.24	300	2003 12 21.26356	20.53	0.02
		wc1221n2065	1.01	300	2003 12 21.33897	20.58	0.02
		wc1221n2066	1.01	300	2003 12 21.34373	20.63	0.02
		wc1223n3027	1.38	300	2003 12 23.23616	20.57	0.02
		wc1223n3028	1.34	300	2003 12 23.24092	20.60	0.02
		wc1223n3044	1.05	300	2003 12 23.30891	20.57	0.02
		wc1223n3045	1.04	300	2003 12 23.31367	20.57	0.02
		wc1223n3057	1.00	300	2003 12 23.37221	20.58	0.02
		wc1223n3058	1.00	300	2003 12 23.37696	20.56	0.02
		wc1223n3076	1.10	320	2003 12 23.43506	20.57	0.02
		wc1223n3077	1.12	320	2003 12 23.44005	20.60	0.02

Table 1—Continued

Name		Image ^a	Airmass	Exp ^b (sec)	UT Date ^c yyyy mm dd.ddddd		Mag. ^d (m_R)	Err (m_R)
(120132)	2003 FY ₁₂₈	wc1223n3084	1.25	320	2003	12 23.47067	20.61	0.02
		wc1223n3085	1.28	320	2003	12 23.47566	20.60	0.02
		wc1224n4026	1.44	300	2003	12 24.22597	20.55	0.02
		wc1224n4027	1.40	300	2003	12 24.23073	20.56	0.02
		wc1224n4035	1.10	300	2003	12 24.28804	20.58	0.02
		wc1224n4036	1.09	300	2003	12 24.29281	20.61	0.02
		wc1224n4043	1.02	300	2003	12 24.32492	20.58	0.02
		wc1224n4044	1.02	300	2003	12 24.32969	20.58	0.02
		wc1224n4053	1.00	300	2003	12 24.37574	20.54	0.02
		wc1224n4054	1.01	300	2003	12 24.38049	20.56	0.02
		wc1224n4063	1.07	350	2003	12 24.42313	20.57	0.02
		wc1224n4076	1.32	300	2003	12 24.47888	20.58	0.02
		wc1224n4077	1.35	300	2003	12 24.48365	20.61	0.02
		fy0309n037	1.16	350	2005	03 09.30416	20.29	0.02
		fy0309n038	1.17	350	2005	03 09.30906	20.31	0.02
		fy0309n045	1.32	350	2005	03 09.34449	20.29	0.02
		fy0309n046	1.35	350	2005	03 09.34942	20.28	0.02
		fy0309n051	1.55	350	2005	03 09.37484	20.28	0.02
		fy0309n052	1.60	350	2005	03 09.37975	20.30	0.02
		fy0310n113	1.37	300	2005	03 10.13114	20.33	0.02
		fy0310n114	1.34	300	2005	03 10.13543	20.31	0.02
		fy0310n121	1.15	300	2005	03 10.18141	20.27	0.02
		fy0310n122	1.14	300	2005	03 10.18572	20.29	0.02
		fy0310n131	1.08	250	2005	03 10.23854	20.28	0.02
		fy0310n132	1.08	250	2005	03 10.24229	20.27	0.02
		fy0310n142	1.17	300	2005	03 10.30636	20.29	0.02
		fy0310n146	1.27	300	2005	03 10.33107	20.27	0.02
		fy0310n147	1.29	300	2005	03 10.33564	20.27	0.02
		fy0310n152	1.51	300	2005	03 10.36726	20.25	0.02
		fy0310n153	1.55	300	2005	03 10.37157	20.22	0.02

Table 1—Continued

Name			Image ^a	Airmass	Exp ^b (sec)	UT Date ^c yyyy mm dd.ddddd	Mag. ^d (m_R)	Err (m_R)
(136199)	Eris	2003 UB ₃₁₃	ub1026c142	1.71	350	2005 10 25.02653	18.372	0.006
			ub1026c143	1.65	350	2005 10 25.03144	18.374	0.005
			ub1026c150	1.37	300	2005 10 25.06369	18.370	0.005
			ub1026c156	1.35	300	2005 10 25.06800	18.361	0.005
			ub1026c162	1.11	250	2005 10 25.19559	18.361	0.005
			ub1026c170	1.11	250	2005 10 25.19931	18.364	0.005
			ub1026c171	1.16	250	2005 10 25.22449	18.360	0.005
			ub1026c174	1.16	250	2005 10 25.22825	18.370	0.005
			ub1026c175	1.25	300	2005 10 25.25305	18.327	0.005
			ub1026c178	1.27	300	2005 10 25.25694	18.365	0.005
			ub1026c179	1.38	300	2005 10 25.27710	18.350	0.005
			ub1026c183	1.41	300	2005 10 25.28146	18.369	0.005
			ub1026c184	1.54	300	2005 10 25.29766	18.365	0.005
			ub1026c187	1.58	300	2005 10 25.30202	18.351	0.005
			ub1026c188	1.78	350	2005 10 25.31871	18.364	0.006
			ub1026c189	1.85	350	2005 10 25.32363	18.364	0.006
			ub1027c043	1.83	250	2005 10 26.01513	18.356	0.006
			ub1027c044	1.78	250	2005 10 26.01890	18.362	0.006
			ub1027c049	1.34	200	2005 10 26.06597	18.360	0.005
			ub1027c050	1.18	300	2005 10 26.10460	18.352	0.005
			ub1027c069	1.10	300	2005 10 26.14440	18.348	0.005
			ub1027c070	1.11	250	2005 10 26.19650	18.352	0.005
			ub1027c074	1.11	250	2005 10 26.20049	18.365	0.005
			ub1027c075	1.15	300	2005 10 26.21742	18.348	0.005
			ub1027c084	1.16	300	2005 10 26.22174	18.359	0.005
			ub1027c085	1.20	300	2005 10 26.23858	18.351	0.005
			ub1027c088	1.22	300	2005 10 26.24295	18.331	0.005
			ub1027c089	1.36	300	2005 10 26.27118	18.352	0.005
			ub1027c092	1.39	300	2005 10 26.27555	18.345	0.005
			ub1027c093	1.51	350	2005 10 26.29210	18.344	0.005

Table 1—Continued

Name	Image ^a	Airmass	Exp ^b (sec)	UT Date ^c yyyy mm dd.ddddd	Mag. ^d (m_R)	Err (m_R)
ub1027c096		1.56	350	2005 10 26.29702	18.345	0.005
ub1027c097		1.61	350	2005 10 26.30193	18.357	0.005
ub1028c240		1.65	300	2005 10 27.02670	18.350	0.005
ub1028c246		1.33	300	2005 10 27.06572	18.362	0.005
ub1028c258		1.10	250	2005 10 27.14482	18.357	0.005
ub1028c266		1.12	250	2005 10 27.19952	18.359	0.005
ub1028c267		1.12	250	2005 10 27.20321	18.367	0.005
ub1028c271		1.18	300	2005 10 27.22789	18.370	0.005
ub1028c272		1.19	300	2005 10 27.23216	18.366	0.005
ub1028c276		1.29	300	2005 10 27.25643	18.272	0.005
ub1028c277		1.31	300	2005 10 27.26070	18.376	0.005
ub1028c280		1.42	300	2005 10 27.27739	18.375	0.005
ub1028c281		1.45	300	2005 10 27.28171	18.369	0.005
ub1028c282		1.48	300	2005 10 27.28598	18.371	0.005
ub1028c283		1.52	300	2005 10 27.29033	18.372	0.005
ub1028c284		1.56	300	2005 10 27.29462	18.371	0.005
ub1028c285		1.61	300	2005 10 27.29900	18.381	0.005
ub1028c286		1.65	300	2005 10 27.30333	18.392	0.005
ub1028c287		1.70	300	2005 10 27.30761	18.393	0.006
ub1028c288		1.76	300	2005 10 27.31197	18.383	0.006
ub1028c289		1.82	300	2005 10 27.31625	18.369	0.006
ub1028c290		1.89	300	2005 10 27.32052	18.388	0.006
ub1028c291		1.96	300	2005 10 27.32484	18.367	0.006
ub1028c292		2.04	300	2005 10 27.32916	18.405	0.007
ub1028c293		2.13	300	2005 10 27.33347	18.378	0.007
ub1128n027		1.11	250	2005 11 28.10847	18.389	0.005
ub1128n028		1.12	250	2005 11 28.11219	18.382	0.005
ub1128n029		1.12	250	2005 11 28.11593	18.401	0.005
ub1128n032		1.16	250	2005 11 28.13378	18.391	0.005
ub1128n033		1.17	250	2005 11 28.13749	18.383	0.005

Table 1—Continued

Name	Image ^a	Airmass	Exp ^b (sec)	UT Date ^c yyyy mm dd.ddddd	Mag. ^d (m_R)	Err (m_R)
ub1128n034		1.18	250	2005 11 28.14118	18.391	0.005
ub1128n035		1.19	250	2005 11 28.14496	18.389	0.005
ub1128n036		1.21	250	2005 11 28.14866	18.386	0.005
ub1128n037		1.22	250	2005 11 28.15236	18.380	0.005
ub1128n038		1.23	250	2005 11 28.15614	18.376	0.005
ub1128n039		1.25	250	2005 11 28.15983	18.397	0.005
ub1128n040		1.27	250	2005 11 28.16353	18.393	0.005
ub1128n041		1.28	250	2005 11 28.16732	18.379	0.005
ub1128n042		1.30	250	2005 11 28.17102	18.378	0.005
ub1128n043		1.32	250	2005 11 28.17472	18.402	0.005
ub1128n044		1.34	250	2005 11 28.17850	18.379	0.005
ub1128n045		1.37	250	2005 11 28.18220	18.385	0.005
ub1128n046		1.39	250	2005 11 28.18589	18.380	0.005
ub1128n047		1.42	250	2005 11 28.18969	18.375	0.005
ub1128n048		1.44	250	2005 11 28.19339	18.387	0.005
ub1128n049		1.47	250	2005 11 28.19708	18.396	0.005
ub1128n050		1.51	250	2005 11 28.20084	18.393	0.005
ub1128n051		1.54	250	2005 11 28.20453	18.390	0.005
ub1128n052		1.58	250	2005 11 28.20822	18.391	0.005
ub1128n053		1.61	250	2005 11 28.21195	18.391	0.005
ub1128n054		1.66	250	2005 11 28.21565	18.376	0.005
ub1128n055		1.70	250	2005 11 28.21935	18.386	0.005
ub1128n056		1.75	250	2005 11 28.22311	18.377	0.006
ub1128n057		1.80	250	2005 11 28.22680	18.379	0.006
ub1128n058		1.85	250	2005 11 28.23050	18.382	0.006
ub1128n059		1.91	250	2005 11 28.23437	18.393	0.006
ub1128n060		1.98	250	2005 11 28.23800	18.386	0.006
ub1128n061		2.05	250	2005 11 28.24173	18.376	0.007
ub1128n062		2.13	250	2005 11 28.24546	18.383	0.007
ub1129n112		1.15	250	2005 11 29.02268	18.424	0.005

Table 1—Continued

Name	Image ^a	Airmass	Exp ^b (sec)	UT Date ^c yyyy mm dd.ddddd	Mag. ^d (m_R)	Err (m_R)
ub1129n119		1.09	250	2005 11 29.08304	18.432	0.005
ub1129n120		1.09	250	2005 11 29.08673	18.429	0.005
ub1129n121		1.10	250	2005 11 29.09043	18.421	0.005
ub1129n122		1.10	250	2005 11 29.09412	18.430	0.005
ub1129n123		1.10	250	2005 11 29.09782	18.426	0.005
ub1129n124		1.11	250	2005 11 29.10161	18.426	0.005
ub1129n125		1.11	250	2005 11 29.10530	18.431	0.005
ub1129n126		1.12	250	2005 11 29.10900	18.435	0.005
ub1129n127		1.12	250	2005 11 29.11269	18.418	0.005
ub1129n128		1.13	250	2005 11 29.11639	18.422	0.005
ub1129n129		1.14	250	2005 11 29.12018	18.435	0.005
ub1129n130		1.14	250	2005 11 29.12387	18.425	0.005
ub1129n131		1.15	250	2005 11 29.12757	18.418	0.005
ub1129n132		1.16	250	2005 11 29.13136	18.421	0.005
ub1129n133		1.17	250	2005 11 29.13506	18.421	0.005
ub1129n134		1.18	250	2005 11 29.13876	18.420	0.005
ub1129n135		1.20	250	2005 11 29.14254	18.415	0.005
ub1129n136		1.21	250	2005 11 29.14624	18.419	0.005
ub1129n137		1.22	250	2005 11 29.14993	18.424	0.005
ub1129n138		1.24	250	2005 11 29.15373	18.426	0.005
ub1129n139		1.25	250	2005 11 29.15742	18.422	0.005
ub1129n142		1.35	250	2005 11 29.17679	18.418	0.005
ub1129n143		1.37	250	2005 11 29.18049	18.421	0.005
ub1129n144		1.40	250	2005 11 29.18418	18.408	0.005
ub1129n145		1.43	250	2005 11 29.18788	18.422	0.005
ub1129n146		1.45	250	2005 11 29.19158	18.397	0.005
ub1129n147		1.48	250	2005 11 29.19531	18.412	0.005
ub1129n148		1.52	250	2005 11 29.19901	18.403	0.005
ub1129n149		1.55	250	2005 11 29.20270	18.394	0.005
ub1129n150		1.59	250	2005 11 29.20640	18.401	0.005

Table 1—Continued

Name	Image ^a	Airmass	Exp ^b (sec)	UT Date ^c yyyy mm dd.ddddd	Mag. ^d (m_R)	Err (m_R)
ub1129n151		1.63	250	2005 11 29.21010	18.400	0.005
ub1129n152		1.67	250	2005 11 29.21388	18.405	0.005
ub1129n153		1.71	250	2005 11 29.21758	18.401	0.005
ub1129n154		1.76	250	2005 11 29.22127	18.391	0.005
ub1129n155		1.81	250	2005 11 29.22496	18.397	0.006
ub1129n156		1.87	250	2005 11 29.22866	18.396	0.006
ub1129n157		1.93	250	2005 11 29.23238	18.415	0.006
ub1129n158		2.00	250	2005 11 29.23607	18.399	0.006
ub1130n226		1.13	250	2005 11 30.11178	18.386	0.005
ub1130n227		1.13	250	2005 11 30.11548	18.386	0.005
ub1130n228		1.14	250	2005 11 30.11918	18.394	0.005
ub1130n229		1.15	250	2005 11 30.12288	18.394	0.005
ub1130n230		1.16	250	2005 11 30.12657	18.390	0.005
ub1130n231		1.17	250	2005 11 30.13027	18.383	0.005
ub1130n232		1.18	250	2005 11 30.13397	18.398	0.005
ub1130n233		1.19	250	2005 11 30.13766	18.394	0.005
ub1130n234		1.20	250	2005 11 30.14136	18.392	0.005
ub1130n235		1.21	250	2005 11 30.14515	18.384	0.005
ub1130n236		1.23	250	2005 11 30.14884	18.391	0.005
ub1130n237		1.24	250	2005 11 30.15254	18.387	0.005
ub1130n238		1.26	250	2005 11 30.15624	18.391	0.005
ub1130n239		1.28	250	2005 11 30.15993	18.397	0.005
ub1130n240		1.29	250	2005 11 30.16370	18.388	0.005
ub1130n241		1.31	250	2005 11 30.16740	18.405	0.005
ub1130n242		1.33	250	2005 11 30.17110	18.379	0.005
ub1130n243		1.36	250	2005 11 30.17480	18.388	0.005
ub1130n244		1.38	250	2005 11 30.17849	18.383	0.005
ub1130n247		1.50	250	2005 11 30.19434	18.386	0.005
ub1130n248		1.53	250	2005 11 30.19804	18.394	0.005
ub1130n249		1.57	250	2005 11 30.20173	18.393	0.005

Table 1—Continued

Name	Image ^a	Airmass	Exp ^b (sec)	UT Date ^c yyyy mm dd.ddddd	Mag. ^d (m_R)	Err (m_R)
ub1130n250		1.60	250	2005 11 30.20543	18.400	0.005
ub1130n251		1.64	250	2005 11 30.20912	18.397	0.005
ub1130n252		1.69	250	2005 11 30.21281	18.390	0.005
ub1130n253		1.73	250	2005 11 30.21651	18.387	0.005
ub1130n254		1.78	250	2005 11 30.22020	18.403	0.006
ub1130n255		1.84	250	2005 11 30.22389	18.399	0.006
ub1130n256		1.90	250	2005 11 30.22768	18.379	0.006
ub1130n257		1.96	250	2005 11 30.23138	18.394	0.006
ub1130n258		2.03	250	2005 11 30.23514	18.393	0.007
ub1201n327		1.10	300	2005 12 01.04542	18.378	0.005
ub1201n333		1.10	250	2005 12 01.08574	18.376	0.005
ub1201n334		1.10	250	2005 12 01.08943	18.397	0.005
ub1201n335		1.10	250	2005 12 01.09313	18.386	0.005
ub1201n338		1.12	250	2005 12 01.10868	18.391	0.005
ub1201n339		1.13	250	2005 12 01.11237	18.381	0.005
ub1201n340		1.14	250	2005 12 01.11606	18.398	0.005
ub1201n341		1.15	250	2005 12 01.11976	18.382	0.005
ub1201n342		1.16	250	2005 12 01.12347	18.385	0.005
ub1201n343		1.17	250	2005 12 01.12725	18.389	0.005
ub1201n344		1.18	250	2005 12 01.13095	18.388	0.005
ub1201n345		1.19	250	2005 12 01.13465	18.386	0.005
ub1201n346		1.20	250	2005 12 01.13843	18.384	0.005
ub1201n347		1.21	250	2005 12 01.14212	18.381	0.005
ub1201n348		1.23	250	2005 12 01.14581	18.381	0.005
ub1201n351		1.30	250	2005 12 01.16207	18.379	0.005
ub1201n352		1.32	250	2005 12 01.16577	18.394	0.005
ub1201n353		1.34	250	2005 12 01.16946	18.394	0.005
ub1201n354		1.36	250	2005 12 01.17316	18.385	0.005
ub1201n355		1.39	250	2005 12 01.17685	18.383	0.005
ub1201n356		1.41	250	2005 12 01.18055	18.391	0.005

Table 1—Continued

Name		Image ^a	Airmass	Exp ^b (sec)	UT Date ^c yyyy mm dd.ddddd	Mag. ^d (m_R)	Err (m_R)
(84922)	2003 VS ₂	ub1201n357	1.44	250	2005 12 01.18424	18.379	0.005
		ub1201n358	1.47	250	2005 12 01.18793	18.377	0.005
		ub1201n359	1.50	250	2005 12 01.19163	18.381	0.005
		ub1201n360	1.53	250	2005 12 01.19548	18.394	0.005
		ub1201n361	1.57	250	2005 12 01.19918	18.389	0.005
		ub1201n362	1.61	250	2005 12 01.20287	18.388	0.005
		ub1201n363	1.65	250	2005 12 01.20688	18.388	0.005
		ub1201n364	1.69	250	2005 12 01.21058	18.377	0.005
		ub1201n365	1.74	250	2005 12 01.21427	18.390	0.006
		ub1201n366	1.79	250	2005 12 01.21797	18.396	0.006
		ub1201n367	1.85	250	2005 12 01.22166	18.396	0.006
		ub1201n368	1.96	250	2005 12 01.22846	18.390	0.007
		ub1201n369	2.03	250	2005 12 01.23228	18.382	0.007
		vs1219n1031	1.07	250	2003 12 19.26838	19.39	0.01
		vs1219n1032	1.06	250	2003 12 19.27266	19.36	0.01
		vs1219n1043	1.02	250	2003 12 19.31376	19.37	0.01
		vs1219n1044	1.02	250	2003 12 19.31810	19.41	0.01
		vs1219n1055	1.03	220	2003 12 19.35203	19.53	0.01
		vs1219n1056	1.04	220	2003 12 19.35594	19.52	0.01
		vs1219n1064	1.11	220	2003 12 19.39432	19.53	0.01
		vs1219n1065	1.12	220	2003 12 19.39821	19.52	0.01
		vs1219n1075	1.29	220	2003 12 19.43959	19.39	0.01
		vs1219n1076	1.31	220	2003 12 19.44346	19.38	0.01
		vs1219n1086	1.67	230	2003 12 19.48544	19.34	0.01
		vs1219n1087	1.72	230	2003 12 19.48944	19.38	0.01
		vs1221n2024	1.26	220	2003 12 21.20617	19.52	0.01
		vs1221n2025	1.24	220	2003 12 21.21014	19.52	0.01
		vs1221n2040	1.10	220	2003 12 21.24958	19.53	0.01
		vs1221n2041	1.09	220	2003 12 21.25340	19.52	0.01
		vs1221n2046	1.05	220	2003 12 21.27486	19.46	0.01

Table 1—Continued

Name			Image ^a	Airmass	Exp ^b (sec)	UT Date ^c yyyy mm dd.ddddd	Mag. ^d (m_R)	Err (m_R)
(90482)	Orcus	2004 DW	vs1221n2047	1.05	220	2003 12 21.27870	19.45	0.01
			vs1223n3022	1.21	200	2003 12 23.21214	19.41	0.01
			vs1223n3023	1.19	200	2003 12 23.21579	19.44	0.01
			vs1223n3024	1.17	250	2003 12 23.22026	19.46	0.01
			vs1223n3042	1.02	220	2003 12 23.30008	19.34	0.01
			vs1223n3043	1.02	220	2003 12 23.30391	19.33	0.01
			vs1223n3055	1.07	220	2003 12 23.36359	19.46	0.01
			vs1223n3056	1.07	220	2003 12 23.36743	19.50	0.01
			vs1223n3074	1.28	220	2003 12 23.42704	19.47	0.01
			vs1223n3075	1.31	220	2003 12 23.43087	19.46	0.01
			vs1223n3082	1.55	200	2003 12 23.46289	19.36	0.01
			vs1223n3083	1.59	200	2003 12 23.46644	19.35	0.01
			vs1224n4022	1.23	250	2003 12 24.20522	19.35	0.01
			vs1224n4023	1.21	250	2003 12 24.20940	19.38	0.01
			vs1224n4030	1.05	220	2003 12 24.26469	19.37	0.01
			vs1224n4031	1.05	220	2003 12 24.26848	19.38	0.01
			vs1224n4039	1.02	220	2003 12 24.30385	19.51	0.01
			vs1224n4040	1.02	220	2003 12 24.30871	19.52	0.01
			vs1224n4049	1.06	220	2003 12 24.35630	19.45	0.01
			vs1224n4050	1.06	220	2003 12 24.36014	19.44	0.01
			vs1224n4059	1.19	220	2003 12 24.40395	19.34	0.01
			vs1224n4060	1.20	220	2003 12 24.40778	19.32	0.01
			vs1224n4070	1.50	220	2003 12 24.45457	19.43	0.01
			vs1224n4071	1.53	220	2003 12 24.45839	19.48	0.01
			dw0214n028	1.22	200	2005 02 14.11873	18.63	0.01
			dw0214n029	1.21	200	2005 02 14.12189	18.65	0.01
			dw0215n106	1.84	250	2005 02 15.03735	18.64	0.01
			dw0215n107	1.78	250	2005 02 15.04156	18.66	0.01
			dw0215n108	1.73	250	2005 02 15.04534	18.65	0.01
			dw0215n109	1.69	250	2005 02 15.04911	18.64	0.01

Table 1—Continued

Name	Image ^a	Airmass	Exp ^b (sec)	UT Date ^c yyyy mm dd.ddddd	Mag. ^d (m_R)	Err (m_R)
dw0215n113		1.42	250	2005 02 15.07806	18.65	0.01
dw0215n114		1.39	250	2005 02 15.08183	18.65	0.01
dw0215n118		1.26	220	2005 02 15.10658	18.65	0.01
dw0215n119		1.25	220	2005 02 15.10998	18.64	0.01
dw0215n128		1.11	220	2005 02 15.17545	18.65	0.01
dw0215n129		1.11	220	2005 02 15.17885	18.65	0.01
dw0215n140		1.18	220	2005 02 15.24664	18.65	0.01
dw0215n141		1.19	220	2005 02 15.25007	18.65	0.01
dw0215n147		1.33	220	2005 02 15.28450	18.63	0.01
dw0215n148		1.35	220	2005 02 15.28789	18.66	0.01
dw0215n155		1.68	230	2005 02 15.32663	18.65	0.01
dw0215n156		1.73	230	2005 02 15.33014	18.64	0.01
dw0216n199		1.76	250	2005 02 16.04005	18.65	0.01
dw0216n200		1.72	250	2005 02 16.04379	18.67	0.01
dw0216n205		1.51	250	2005 02 16.06390	18.66	0.01
dw0216n206		1.47	250	2005 02 16.06767	18.67	0.01
dw0216n209		1.37	250	2005 02 16.08251	18.65	0.01
dw0216n210		1.35	250	2005 02 16.08625	18.66	0.01
dw0216n217		1.17	250	2005 02 16.13055	18.66	0.01
dw0216n218		1.16	250	2005 02 16.13437	18.66	0.01
dw0216n235		1.21	250	2005 02 16.25223	18.64	0.01
dw0216n247		1.81	300	2005 02 16.33285	18.66	0.01
dw0309n014		1.21	250	2005 03 09.05919	18.71	0.01
dw0309n015		1.20	250	2005 03 09.06295	18.70	0.01
dw0309n022		1.11	300	2005 03 09.11334	18.72	0.01
dw0309n023		1.11	300	2005 03 09.11762	18.71	0.01
dw0309n027		1.11	300	2005 03 09.13928	18.69	0.01
dw0309n028		1.11	300	2005 03 09.14363	18.70	0.01
dw0310n091		1.43	250	2005 03 10.01315	18.71	0.01
dw0310n092		1.40	250	2005 03 10.01688	18.71	0.01

Table 1—Continued

Name		Image ^a	Airmass	Exp ^b (sec)	UT Date ^c yyyy mm dd.ddddd	Mag. ^d (m_R)	Err (m_R)
(90568)	2004 GV ₉	dw0310n097	1.27	250	2005 03 10.04113	18.72	0.01
		dw0310n098	1.25	250	2005 03 10.04487	18.72	0.01
		dw0310n107	1.12	250	2005 03 10.09569	18.71	0.01
		dw0310n108	1.12	250	2005 03 10.09945	18.72	0.01
		dw0310n125	1.26	250	2005 03 10.20552	18.70	0.01
		dw0310n126	1.28	250	2005 03 10.20927	18.71	0.01
		dw0310n135	1.67	300	2005 03 10.26076	18.72	0.01
		gv0215n130	1.75	250	2005 02 15.18402	19.75	0.03
		gv0215n131	1.70	250	2005 02 15.18792	19.81	0.03
		gv0215n142	1.19	250	2005 02 15.25502	19.77	0.03
		gv0215n143	1.17	250	2005 02 15.25891	19.73	0.03
		gv0215n153	1.03	250	2005 02 15.31558	19.74	0.03
		gv0215n154	1.03	250	2005 02 15.31931	19.79	0.03
		gv0215n159	1.00	250	2005 02 15.34893	19.77	0.03
		gv0215n160	1.00	250	2005 02 15.35268	19.80	0.03
		gv0215n165	1.01	250	2005 02 15.38618	19.79	0.03
		gv0215n166	1.02	250	2005 02 15.38992	19.83	0.03
		gv0216n229	1.41	250	2005 02 16.21394	19.74	0.03
		gv0216n230	1.38	250	2005 02 16.21768	19.76	0.03
		gv0216n242	1.05	300	2005 02 16.29937	19.76	0.03
		gv0216n254	1.01	300	2005 02 16.37745	19.75	0.03
		gv0309n029	1.46	300	2005 03 09.14960	19.64	0.02
		gv0309n030	1.42	300	2005 03 09.15392	19.66	0.02
		gv0309n033	1.01	300	2005 03 09.27972	19.75	0.02
		gv0309n034	1.00	300	2005 03 09.28405	19.73	0.02
		gv0309n039	1.01	300	2005 03 09.31533	19.70	0.02
		gv0309n040	1.01	300	2005 03 09.31965	19.67	0.02
		gv0309n047	1.06	300	2005 03 09.35654	19.70	0.02
		gv0309n048	1.07	300	2005 03 09.36090	19.68	0.02
		gv0309n054	1.18	300	2005 03 09.39525	19.68	0.02

Table 1—Continued

Name		Image ^a	Airmass	Exp ^b (sec)	UT Date ^c yyyy mm dd.ddddd	Mag. ^d (m_R)	Err (m_R)
(120348)	2004 TY ₃₆₄	gv0309n055	1.20	300	2005 03 09.39959	19.69	0.02
		gv0310n115	1.51	300	2005 03 10.14103	19.64	0.02
		gv0310n116	1.44	300	2005 03 10.14905	19.66	0.02
		gv0310n127	1.11	300	2005 03 10.21489	19.64	0.02
		gv0310n128	1.09	300	2005 03 10.21918	19.68	0.02
		gv0310n143	1.01	300	2005 03 10.31197	19.75	0.02
		gv0310n148	1.04	300	2005 03 10.34106	19.72	0.02
		gv0310n149	1.05	300	2005 03 10.34539	19.77	0.02
		gv0310n155	1.14	300	2005 03 10.38172	19.76	0.02
		gv0310n158	1.20	300	2005 03 10.39711	19.72	0.02
		gv0310n159	1.22	300	2005 03 10.40147	19.73	0.02
		ty1025n041	1.89	400	2005 10 25.01425	19.89	0.01
		ty1025n042	1.81	400	2005 10 25.01944	19.86	0.01
		ty1025n047	1.45	400	2005 10 25.05162	19.87	0.01
		ty1025n048	1.41	400	2005 10 25.05711	19.92	0.01
		ty1025n067	1.04	350	2005 10 25.18450	19.98	0.01
		ty1025n068	1.04	350	2005 10 25.18939	19.99	0.01
		ty1025n072	1.06	350	2005 10 25.21357	19.95	0.01
		ty1025n073	1.07	350	2005 10 25.21847	19.92	0.01
		ty1025n082	1.12	350	2005 10 25.24193	19.89	0.01
		ty1025n083	1.13	350	2005 10 25.24683	19.90	0.01
		ty1025n086	1.19	350	2005 10 25.26632	19.90	0.01
		ty1025n087	1.21	350	2005 10 25.27123	19.90	0.01
		ty1025n090	1.29	350	2005 10 25.28657	19.89	0.01
		ty1025n091	1.32	350	2005 10 25.29147	19.95	0.01
		ty1025n094	1.42	350	2005 10 25.30718	19.95	0.01
		ty1025n095	1.46	350	2005 10 25.31207	20.00	0.01
		ty1025n098	1.63	350	2005 10 25.32928	19.98	0.01
		ty1025n099	1.69	350	2005 10 25.33418	19.97	0.01
		ty1025n100	1.76	350	2005 10 25.33909	20.02	0.01

Table 1—Continued

Name	Image ^a	Airmass	Exp ^b (sec)	UT Date ^c yyyy mm dd.ddddd	Mag. ^d (m_R)	Err (m_R)
ty1025n101		1.83	350	2005 10 25.34410	20.03	0.01
ty1026n144		1.71	400	2005 10 26.02367	19.85	0.01
ty1026n145		1.64	400	2005 10 26.02917	19.86	0.01
ty1026n151		1.30	350	2005 10 26.07121	20.02	0.01
ty1026n157		1.13	400	2005 10 26.11043	20.07	0.01
ty1026n163		1.06	400	2005 10 26.14943	20.03	0.01
ty1026n172		1.06	400	2005 10 26.20516	19.92	0.01
ty1026n176		1.09	400	2005 10 26.22689	19.88	0.01
ty1026n177		1.10	400	2005 10 26.23234	19.90	0.01
ty1026n181		1.16	450	2005 10 26.25425	19.94	0.01
ty1026n182		1.19	450	2005 10 26.26393	19.92	0.01
ty1026n185		1.27	400	2005 10 26.28048	19.95	0.01
ty1026n186		1.30	400	2005 10 26.28599	19.98	0.01
ty1026n190		1.45	450	2005 10 26.30748	20.03	0.01
ty1026n191		1.50	450	2005 10 26.31356	20.09	0.01
ty1026n192		1.56	450	2005 10 26.31963	20.09	0.01
ty1026n193		1.62	450	2005 10 26.32568	20.07	0.01
ty1026n194		1.70	450	2005 10 26.33173	20.09	0.01
ty1026n195		1.78	450	2005 10 26.33774	20.10	0.01
ty1026n196		1.87	450	2005 10 26.34378	20.08	0.01
ty1027n241		1.58	400	2005 10 27.03210	20.01	0.01
ty1027n247		1.28	400	2005 10 27.07100	20.04	0.01
ty1027n264		1.05	400	2005 10 27.18749	19.89	0.01
ty1027n265		1.05	400	2005 10 27.19292	19.87	0.01
ty1027n269		1.07	400	2005 10 27.21551	19.91	0.01
ty1027n270		1.08	400	2005 10 27.22094	19.90	0.01
ty1027n274		1.14	400	2005 10 27.24440	19.90	0.01
ty1027n275		1.15	400	2005 10 27.24988	19.89	0.01
ty1027n278		1.22	350	2005 10 27.26622	19.98	0.01
ty1027n279		1.24	350	2005 10 27.27115	19.99	0.01

Table 1—Continued

Name	Image ^a	Airmass	Exp ^b (sec)	UT Date ^c yyyy mm dd.ddddd	Mag. ^d (m_R)	Err (m_R)
ty1027n294		1.83	400	2005 10 27.33881	20.09	0.01
ty1027n295		1.92	400	2005 10 27.34429	20.09	0.01
ty1027n296		2.02	400	2005 10 27.34976	20.10	0.01
ty1128n030		1.07	350	2005 11 28.12175	19.99	0.01
ty1128n031		1.07	350	2005 11 28.12665	19.99	0.01
ty1128n063		1.87	400	2005 11 28.25204	20.17	0.01
ty1128n064		1.96	400	2005 11 28.25747	20.15	0.01
ty1129n117		1.05	350	2005 11 29.07101	20.00	0.01
ty1129n118		1.04	350	2005 11 29.07586	20.00	0.01
ty1129n140		1.17	350	2005 11 29.16375	20.11	0.01
ty1129n141		1.19	350	2005 11 29.16860	20.12	0.01
ty1129n159		1.76	350	2005 11 29.24196	20.17	0.01
ty1129n160		1.83	350	2005 11 29.24682	20.13	0.01
ty1129n161		1.91	350	2005 11 29.25167	20.15	0.01
ty1129n162		1.99	350	2005 11 29.25657	20.08	0.01
ty1130n224		1.05	350	2005 11 30.10029	19.98	0.01
ty1130n225		1.05	350	2005 11 30.10514	20.00	0.01
ty1130n245		1.27	350	2005 11 30.18325	20.18	0.01
ty1130n246		1.30	350	2005 11 30.18810	20.15	0.01
ty1130n259		1.77	350	2005 11 30.23992	20.12	0.01
ty1130n260		1.84	350	2005 11 30.24478	20.10	0.01
ty1130n261		1.92	350	2005 11 30.24963	20.13	0.01
ty1130n262		2.01	350	2005 11 30.25454	20.11	0.01
ty1201n328		1.06	400	2005 12 01.05104	19.99	0.01
ty1201n336		1.05	350	2005 12 01.09816	20.08	0.01
ty1201n337		1.05	350	2005 12 01.10301	20.07	0.01
ty1201n349		1.14	350	2005 12 01.15006	20.18	0.01
ty1201n350		1.16	350	2005 12 01.15492	20.13	0.01
ty1201n370		1.77	350	2005 12 01.23777	20.05	0.01
ty1201n371		1.85	350	2005 12 01.24262	20.07	0.01

Table 1—Continued

Name	Image ^a	Airmass	Exp ^b (sec)	UT Date ^c yyyy mm dd.ddddd	Mag. ^d (m_R)	Err (m_R)
	ty1201n372	1.93	350	2005 12 01.24748	20.08	0.01
	ty1201n373	2.02	350	2005 12 01.25239	20.04	0.01

^aImage number.

^bExposure time for the image.

^cDecimal Universal Date at the start of the integration.

^dApparent red magnitude.

^eUncertainties on the individual photometric measurements.

Table 2. Properties of Observed KBOs

Name		H^a (mag)	m_R^b (mag)	Nights ^c (#)	Δm_R^d (mag)	Single ^e (hrs)	Double ^f (hrs)
	2001 UQ ₁₈	5.4	22.3	2	< 0.3	-	-
(126154)	2001 YH ₁₄₀	5.4	20.85	4	0.21 ± 0.04	13.25 ± 0.2	-
(55565)	2002 AW ₁₉₇	3.3	19.88	2	< 0.03	-	-
(119979)	2002 WC ₁₉	5.1	20.58	4	< 0.05	-	-
(120132)	2003 FY ₁₂₈	5.0	20.28	2	< 0.08	-	-
(136199)	Eris 2003 UB ₃₁₃	-1.2	18.36	7	< 0.01	-	-
(84922)	2003 VS ₂	4.2	19.45	4	0.21 ± 0.02	-	7.41 ± 0.02
(90482)	Orcus 2004 DW	2.3	18.65	5	< 0.03	-	-
(90568)	2004 GV ₉	4.0	19.68	4	< 0.08	-	-
(120348)	2004 TY ₃₆₄	4.5	19.98	7	0.22 ± 0.02	5.85 ± 0.01	11.70 ± 0.01

^aThe visible absolute magnitude of the object from the Minor Planet Center. The values from the MPC differ than the R-band absolute magnitudes found for the few objects in which we have actual phase curves as shown in Table 3.

^bMean red magnitude of the object. For the four objects observed at significantly different phase angles the data near the lowest phase angle is used: Eris in Oct. 2005, Orcus in Feb. 2005, 90568 in Mar. 2005, and 120348 in Oct. 2005.

^cNumber of nights data were taken to determine the lightcurve.

^dThe peak to peak range of the lightcurve.

^eThe lightcurve period if there is one maximum per period.

^fThe lightcurve period if there are two maximum per period.

Table 3. Phase Function Data for KBOs

Name			$m_R(1, 1, 0)^a$ (mag)	H^b (mag)	MPC ^c (mag)	$\beta(\alpha < 2^\circ)^d$ (mag/deg)
(136199)	Eris	2003 UB ₃₁₃	-1.50 ± 0.02	-1.50 ± 0.02	-1.65	0.09 ± 0.03
(90482)	Orcus	2004 DW	1.81 ± 0.05	1.81 ± 0.05	1.93	0.26 ± 0.05
(90568)		2004 GV ₉	3.64 ± 0.06	3.62 ± 0.06	3.5	0.18 ± 0.06
(120348)		2004 TY ₃₆₄	3.91 ± 0.03	3.90 ± 0.03	4.0	0.19 ± 0.03

^aThe R-band reduced magnitude determined from the linear phase coefficient found in this work.

^bThe R-band absolute magnitude determined as described in *Bowell et al. (1989)*.

^cThe R-band absolute magnitude from the Minor Planet Center converted from the V-band as is shown in Table 2 to the R-band using the known colors of the objects: V-R= 0.45 for Eris (*Brown et al. 2005*), V-R= 0.37 for Orcus (*de Bergh et al. 2005*), and a nominal value of V-R= 0.5 for 90568 and 120348 since these objects don’t have known V-R colors.

^d $\beta(\alpha < 2^\circ)$ is the phase coefficient in magnitudes per degree at phase angles $< 2^\circ$.

Table 4. Phase Function Correlations

β vs. ^a	r_{corr} ^b	N ^c	Sig ^d
$m_R(1, 1, 0)$	0.50	19	97%
$m_V(1, 1, 0)$	0.54	16	97%
$m_I(1, 1, 0)$	0.12	14	< 60%
p_R	-0.51	5	65%
p_V	-0.38	9	70%
p_I	-0.27	10	< 60%
Δm	-0.21	19	< 60%
$B - I$	-0.20	11	< 60%

^a β is the linear phase coefficient in magnitudes per degree at phase angles $< 2^\circ$. In the column are what β is compared to in order to see if there is any correlation; $m_R(1, 1, 0)$, $m_V(1, 1, 0)$ and $m_I(1, 1, 0)$ are the reduced magnitudes in the R, V and I-band respectively and are compared to the value of β determined at the same wavelength; p_R , p_V and p_I are the geometric albedos compared to β in the R, V and I-band respectively; Δm is the peak-to-peak amplitude of the rotational light curve; and $B - I$ is the color. The phase curves in the R-band are from this work and Sheppard and Jewitt (2002;2003) while the V and I-band data are from Buie et al. (1997) and Rabinowitz et al. (2007). The albedo information is from Cruikshank et al. (2006) and the colors from Barucci et al. (2005).

^b r_{corr} is the Pearson correlation coefficient.

^cN is the number of TNOs used for the correlation.

^dSig is the confidence of significance of the correlation.

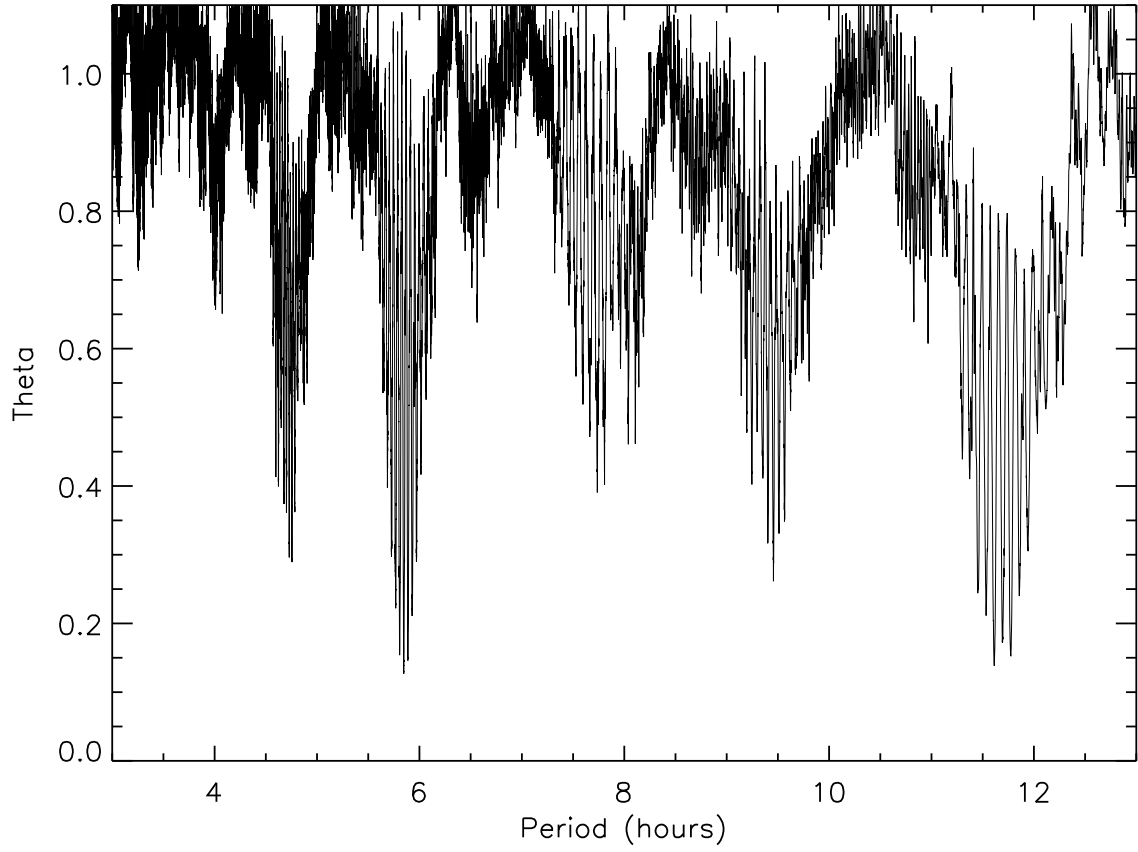


Fig. 1.— The Phase Dispersion Minimization (PDM) plot for (120348) 2004 TY₃₆₄. The best fit single-peaked period is near 5.85 hours.

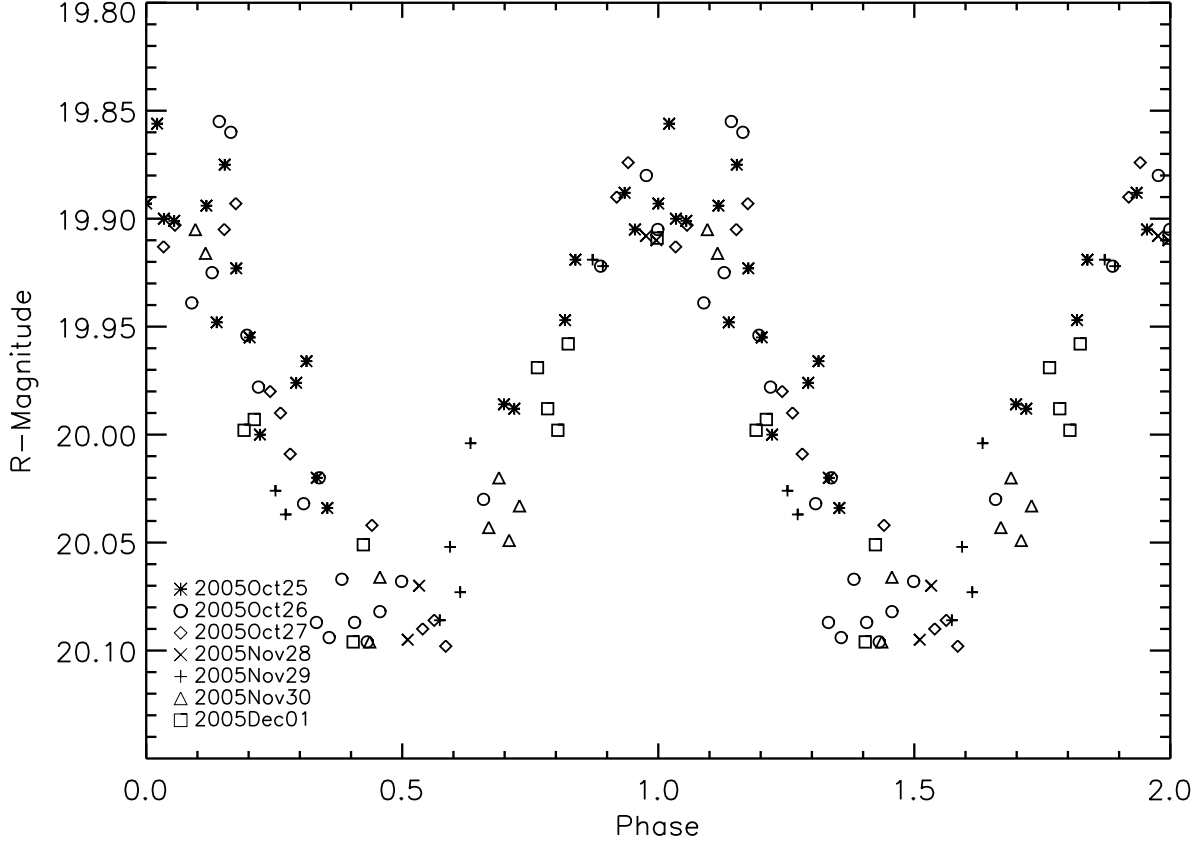


Fig. 2.— The phased best fit single-peaked period for (120348) 2004 TY₃₆₄ of 5.85 hours. The peak-to-peak amplitude is about 0.22 magnitudes. The data from November and December has been vertically shifted to correspond to the same phase angle as the data from October using the phase function found for this object in this work. Individual error bars for the measurements are not shown for clarity but are generally ± 0.01 mags as seen in Table 1.

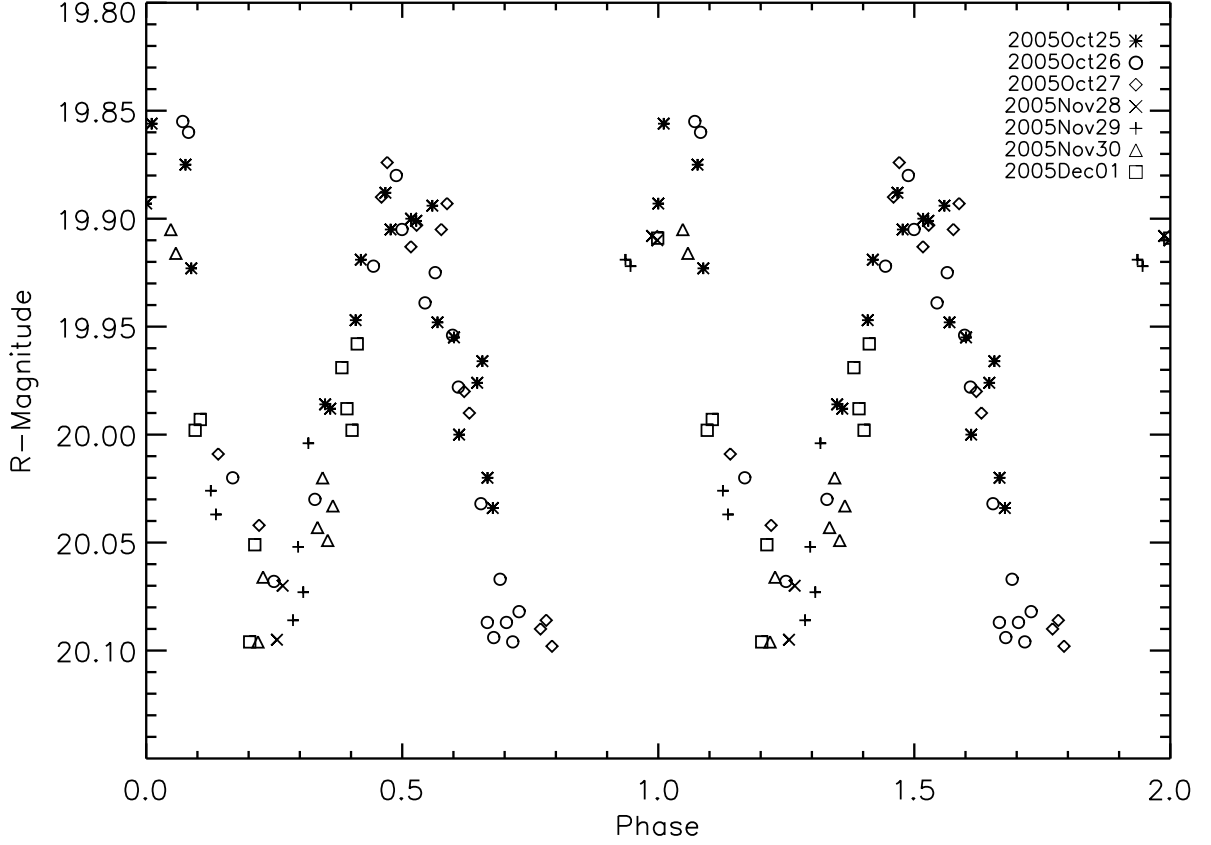


Fig. 3.— The phased double-peaked period for (120348) 2004 TY₃₆₄ of 11.70 hours. The data from November and December has been vertically shifted to correspond to the same phase angle as the data from October using the phase function found for this object in this work. Individual error bars for the measurements are not shown for clarity but are generally ± 0.01 mags as seen in Table 1.

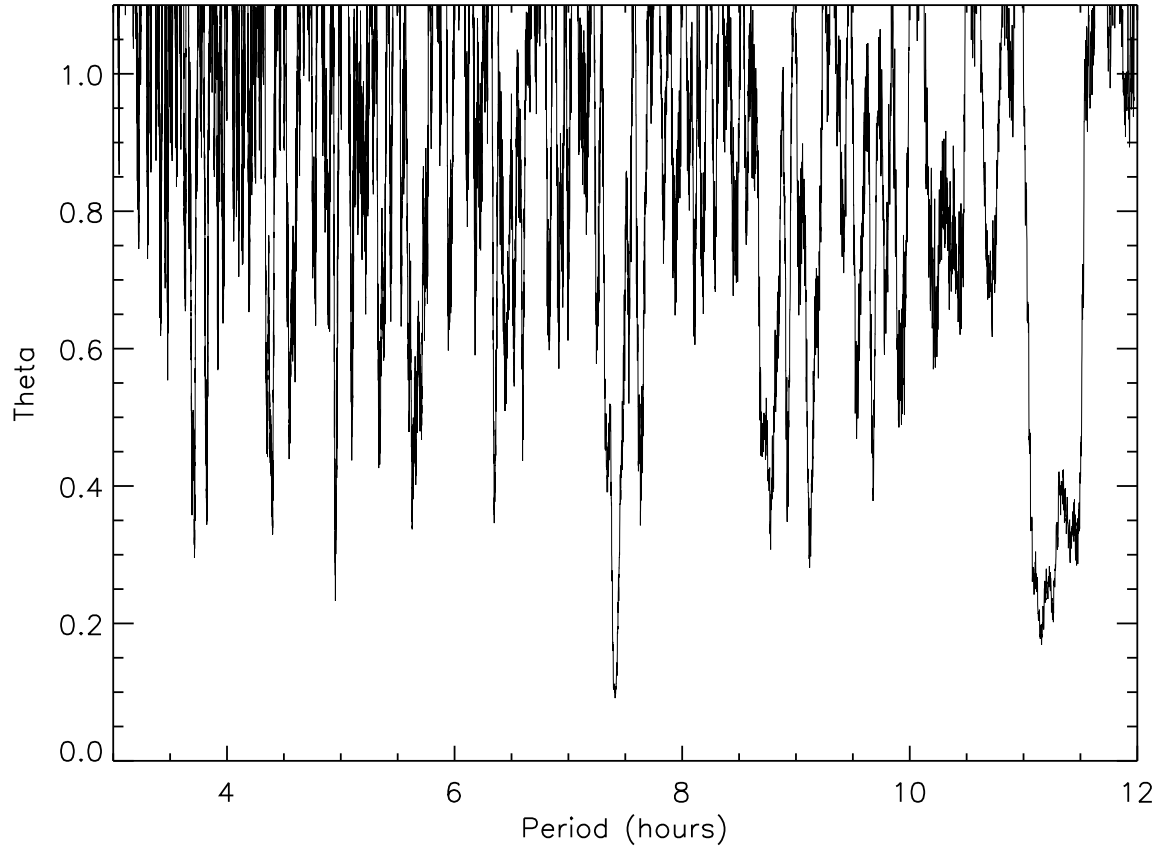


Fig. 4.— The Phase Dispersion Minimization (PDM) plot for (84922) 2003 VS₂. The best fit is the double-peaked period near 7.41 hours.

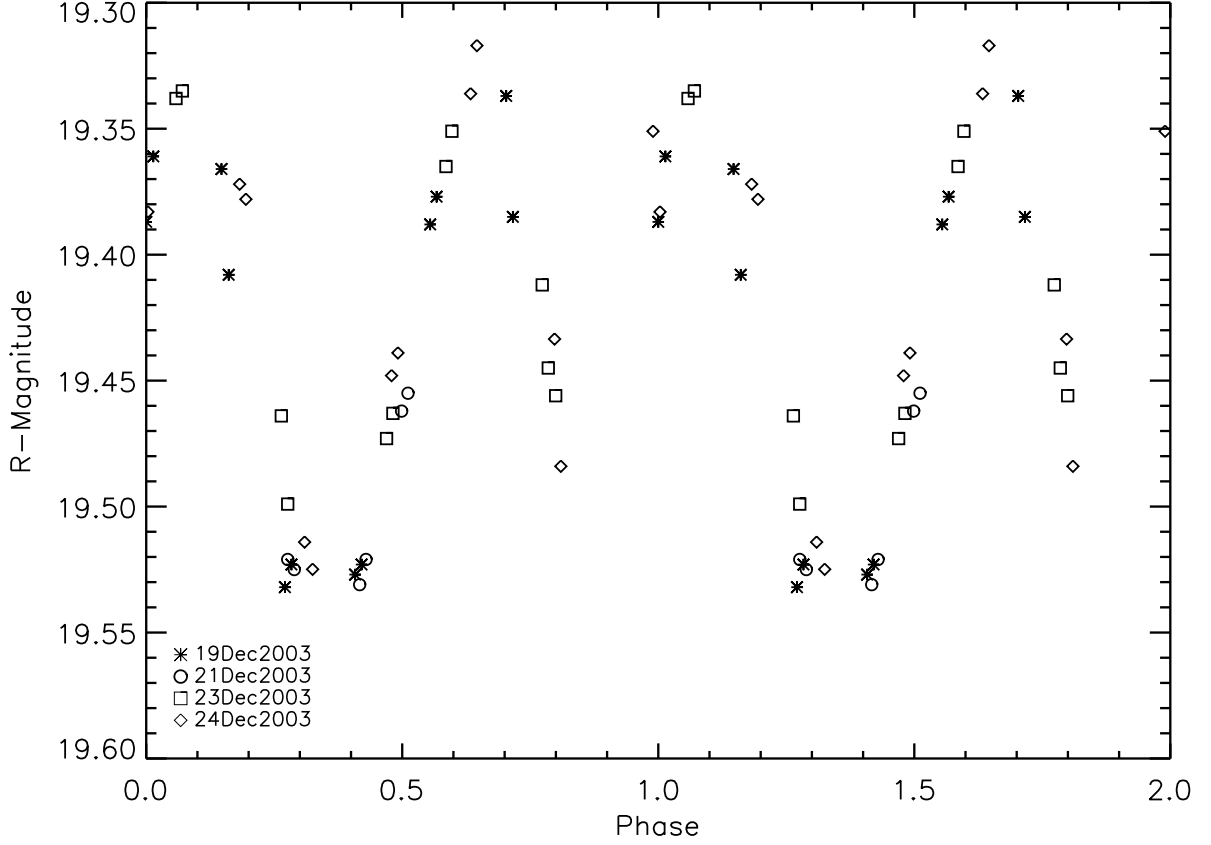


Fig. 5.— The phased best fit double-peaked period for (84922) 2003 VS₂ of 7.41 hours. The peak-to-peak amplitude is about 0.21 magnitudes. The two peaks have differences since one is slightly wider while the other is slightly shorter in amplitude. This is the best fit period for (84922) 2003 VS₂. Individual error bars for the measurements are not shown for clarity but are generally ± 0.01 mags as seen in Table 1.

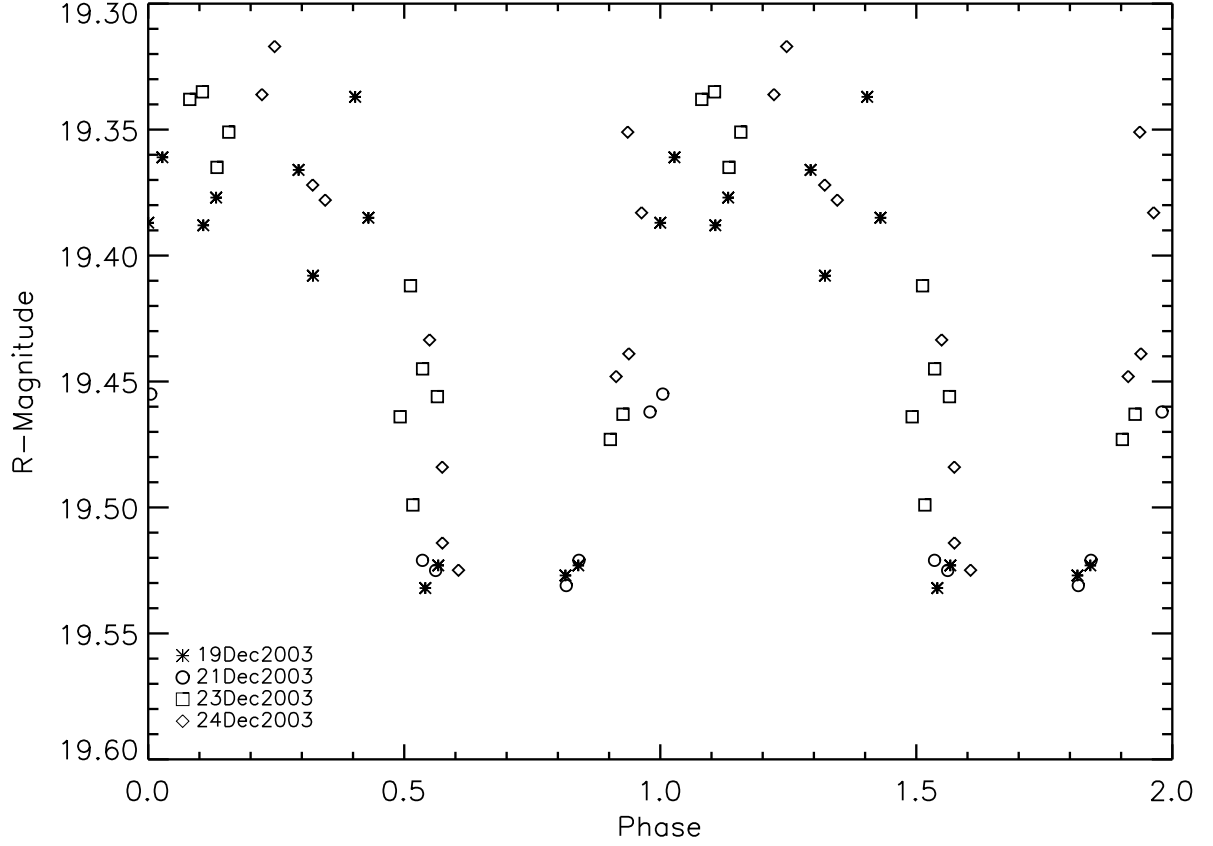


Fig. 6.— The phased single-peaked period for (84922) 2003 VS₂ of 3.70 hours. The single peaked period for 2003 VS₂ does not look well matched and has a larger scatter about the solution compared to the double-peaked period shown in Figure 5. Individual error bars for the measurements are not shown for clarity but are generally ± 0.01 mags as seen in Table 1.

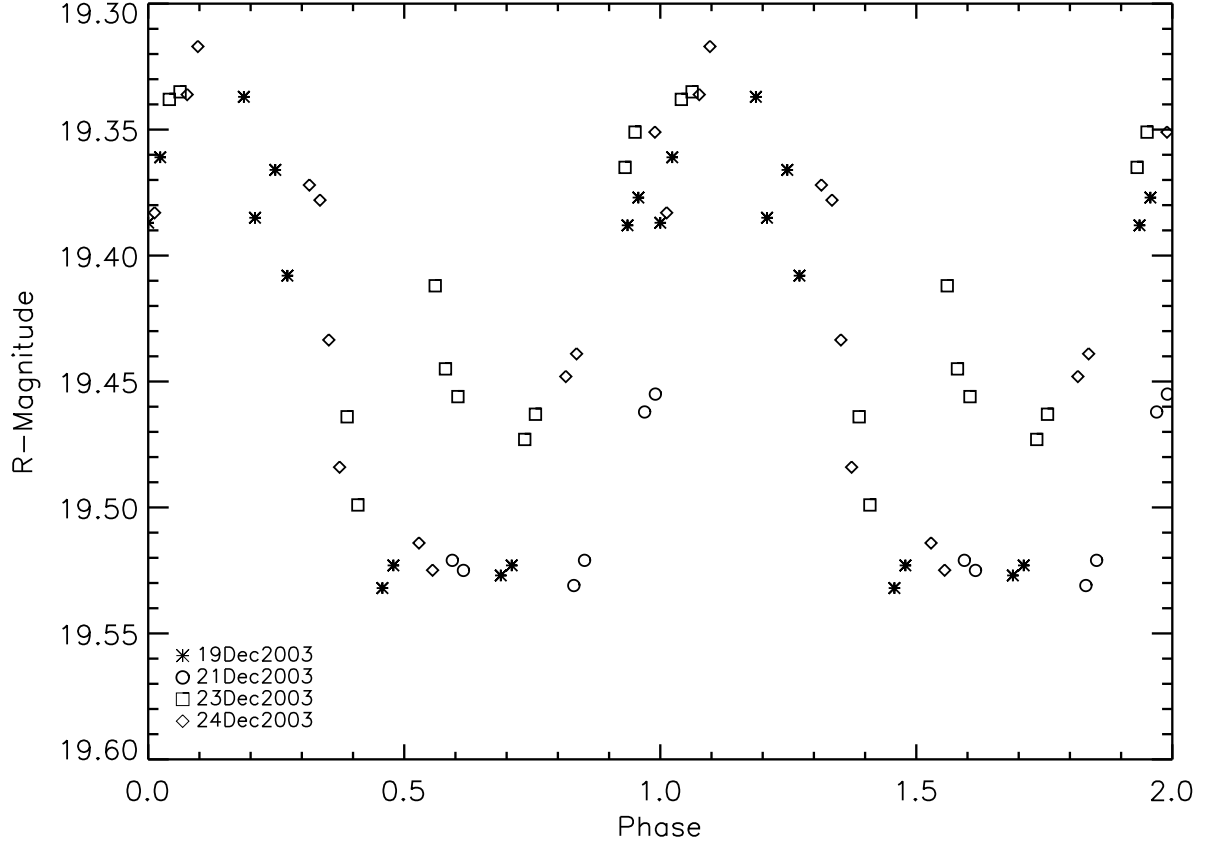


Fig. 7.— The phased single-peaked period for (84922) 2003 VS₂ of 4.39 hours. Again, the single peaked period for 2003 VS₂ does not look well matched and has a larger scatter about the solution compared to the double-peaked period shown in Figure 5. Individual error bars for the measurements are not shown for clarity but are generally ± 0.01 mags as seen in Table 1.

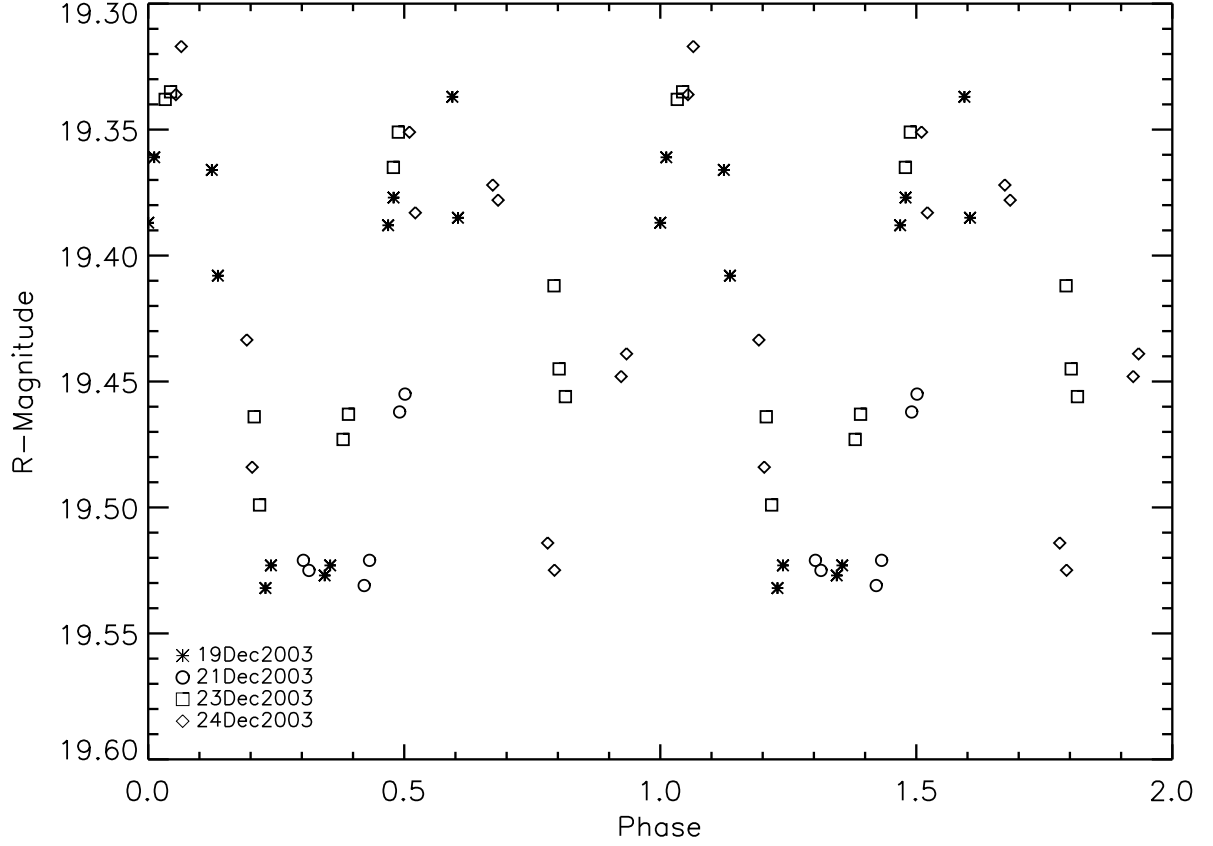


Fig. 8.— The phased double-peaked period for (84922) 2003 VS₂ of 8.77 hours. This double-peaked period for 2003 VS₂ does not look well matched and has a larger scatter about the solution compared to the 7.41 hour double-peaked period shown in Figure 5. Individual error bars for the measurements are not shown for clarity but are generally ± 0.01 mags as seen in Table 1.

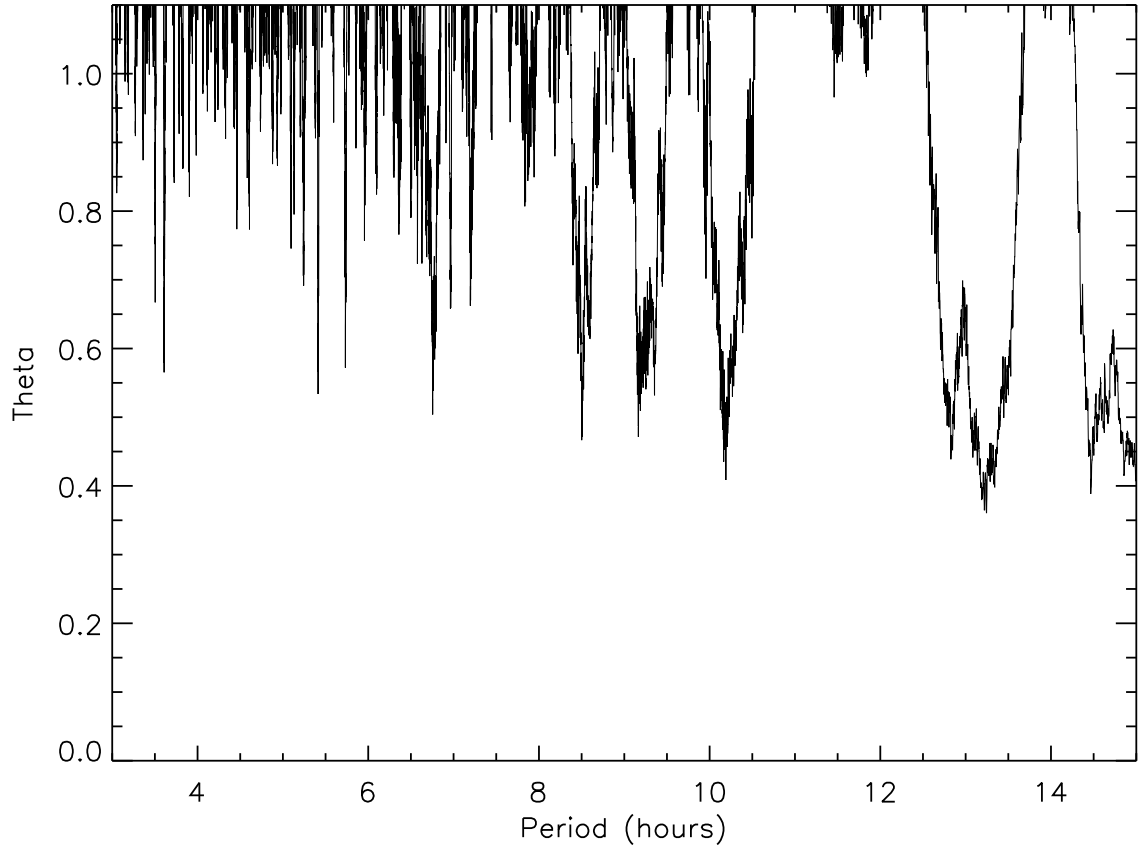


Fig. 9.— The Phase Dispersion Minimization (PDM) plot for 2001 YH₁₄₀. The best fit is the single-peaked period near 13.25 hours. The other possible fits near 8.5, 9.15 and 10.25 hours don't look good when phasing the data and viewing the result by eye.

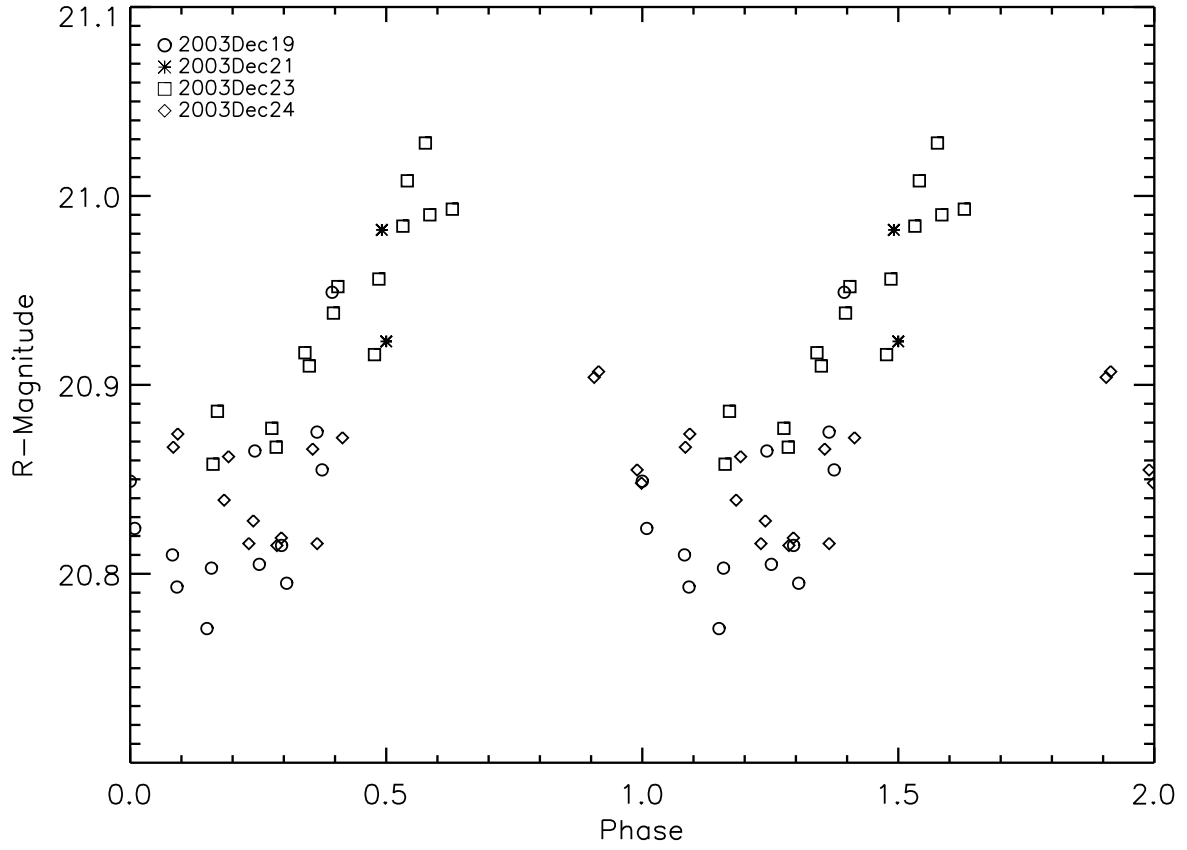


Fig. 10.— The phased best fit single-peaked period for 2001 YH₁₄₀ of 13.25 hours. The peak-to-peak amplitude is about 0.21 magnitudes. Individual error bars for the measurements are not shown for clarity but are generally ± 0.02 mags as seen in Table 1.

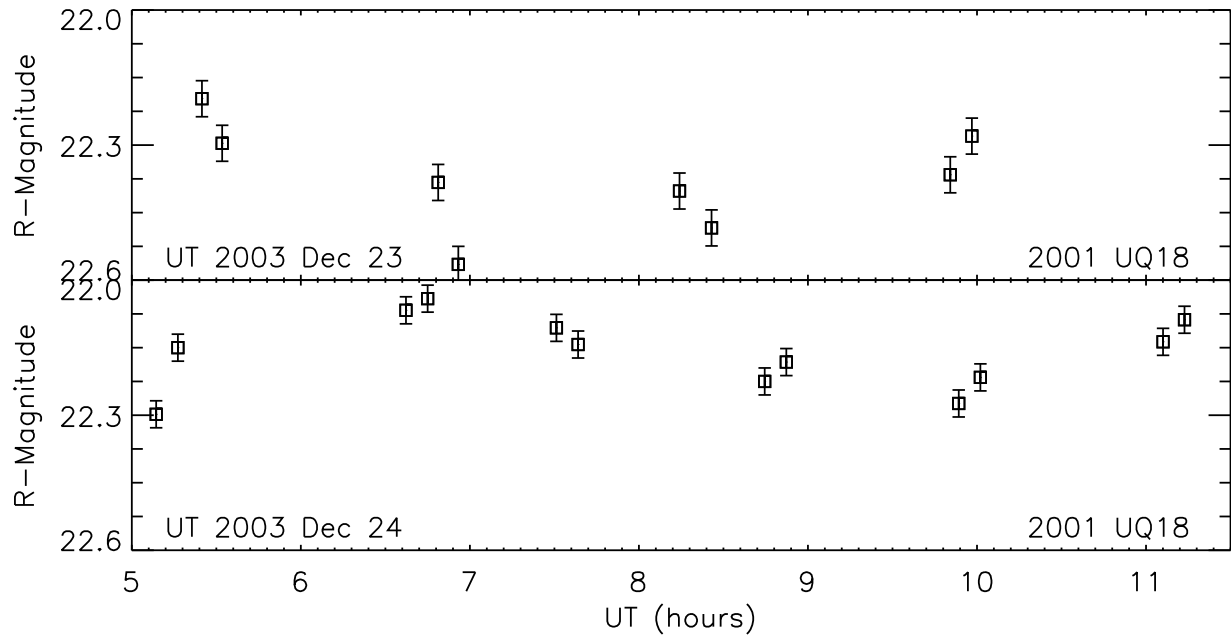


Fig. 11.— The flat light curve of 2001 UQ₁₈. The KBO may have a significant amplitude light curve but further observations are needed to confirm.

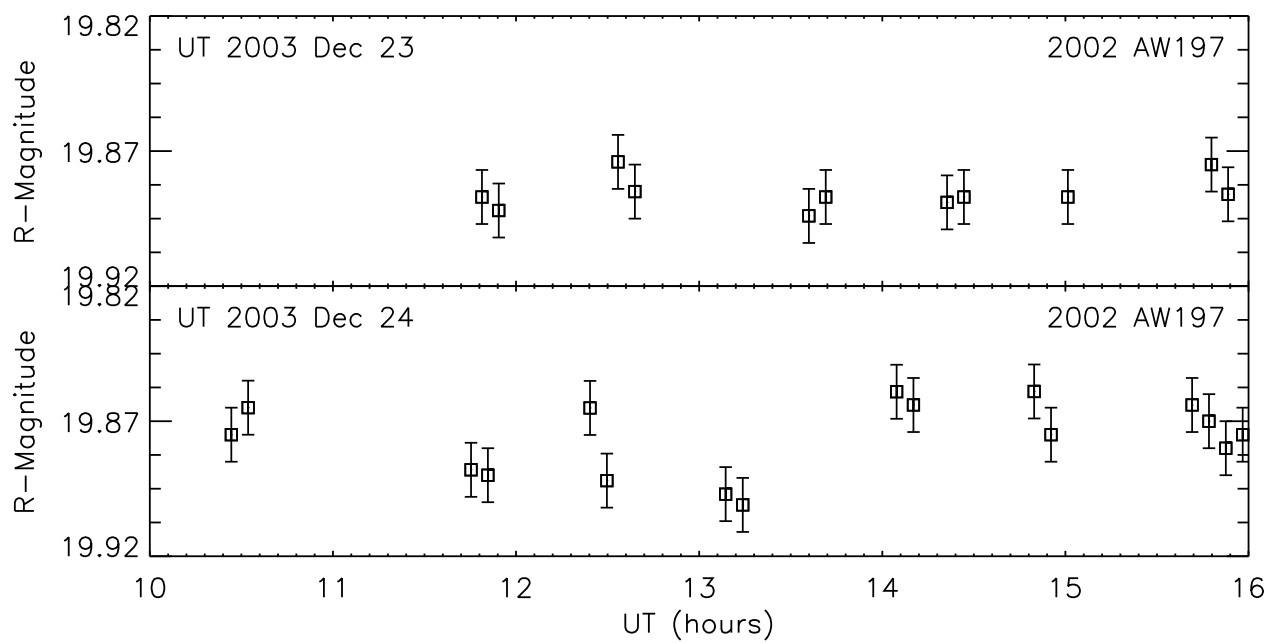


Fig. 12.— The flat light curve of (55565) 2002 AW₁₉₇. The KBO has no significant short-term variations larger than 0.03 magnitudes over two days.

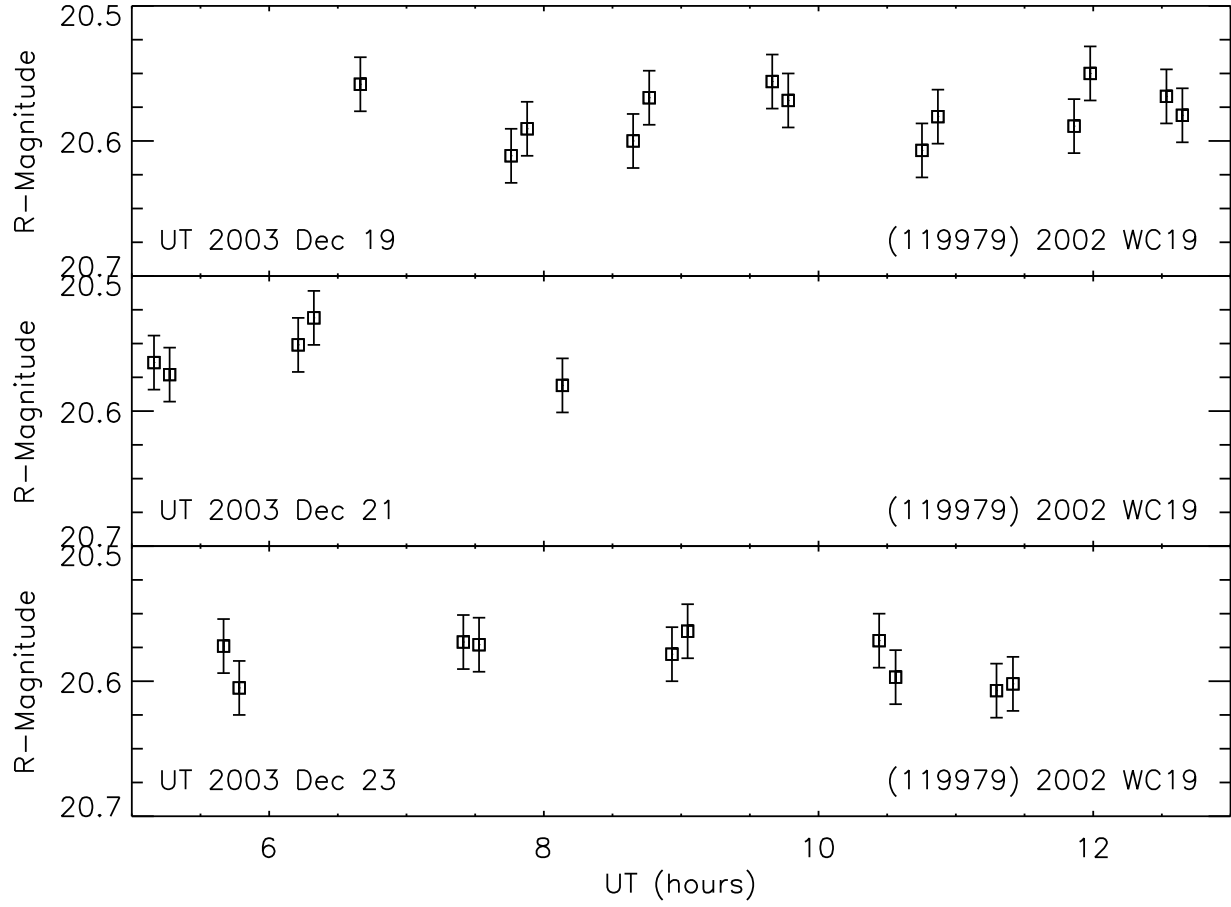


Fig. 13.— The flat light curve of (119979) 2002 WC₁₉. The KBO has no significant short-term variations larger than 0.03 magnitudes over four days.

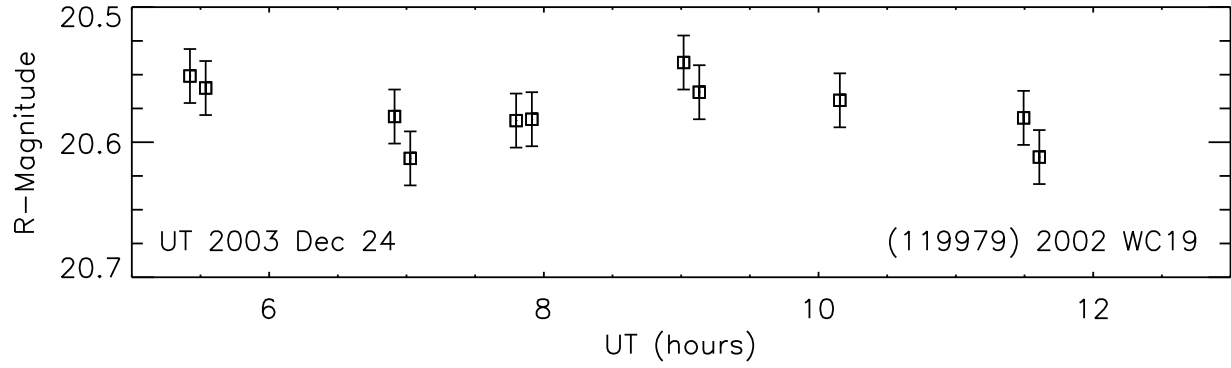


Fig. 14.— The flat light curve of (119979) 2002 WC₁₉. The KBO has no significant short-term variations larger than 0.03 magnitudes over four days.

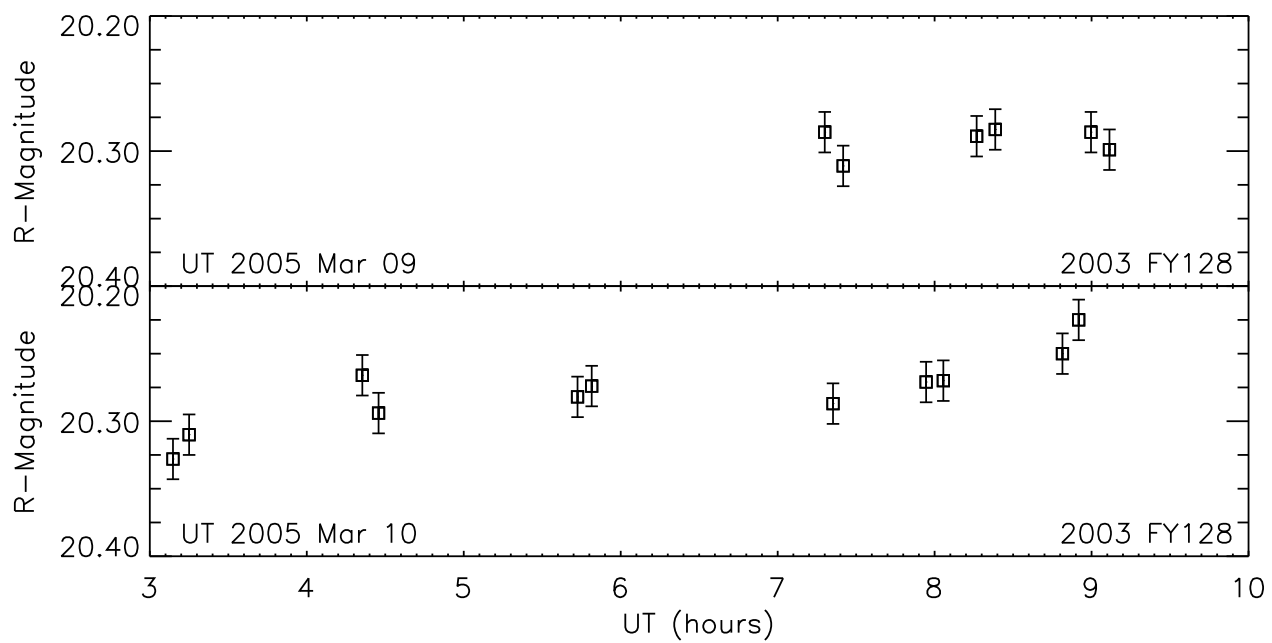


Fig. 15.— The flat light curve of (120132) 2003 FY₁₂₈. The KBO has no significant short-term variations larger than 0.08 magnitudes over two days.

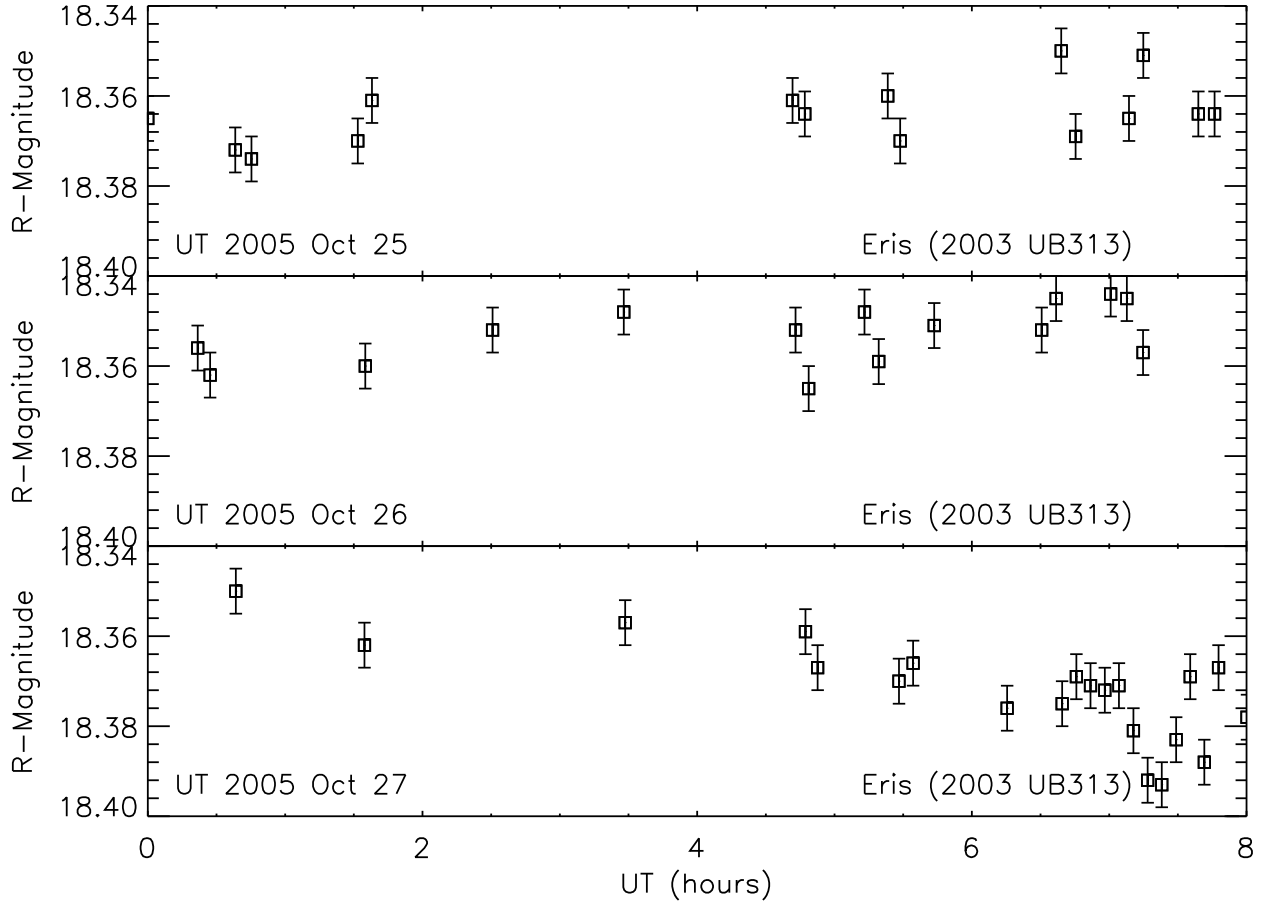


Fig. 16.— The flat light curve of Eris (2003 UB₃₁₃) in October 2005. The KBO has no significant short-term variations larger than 0.01 magnitudes over several days.

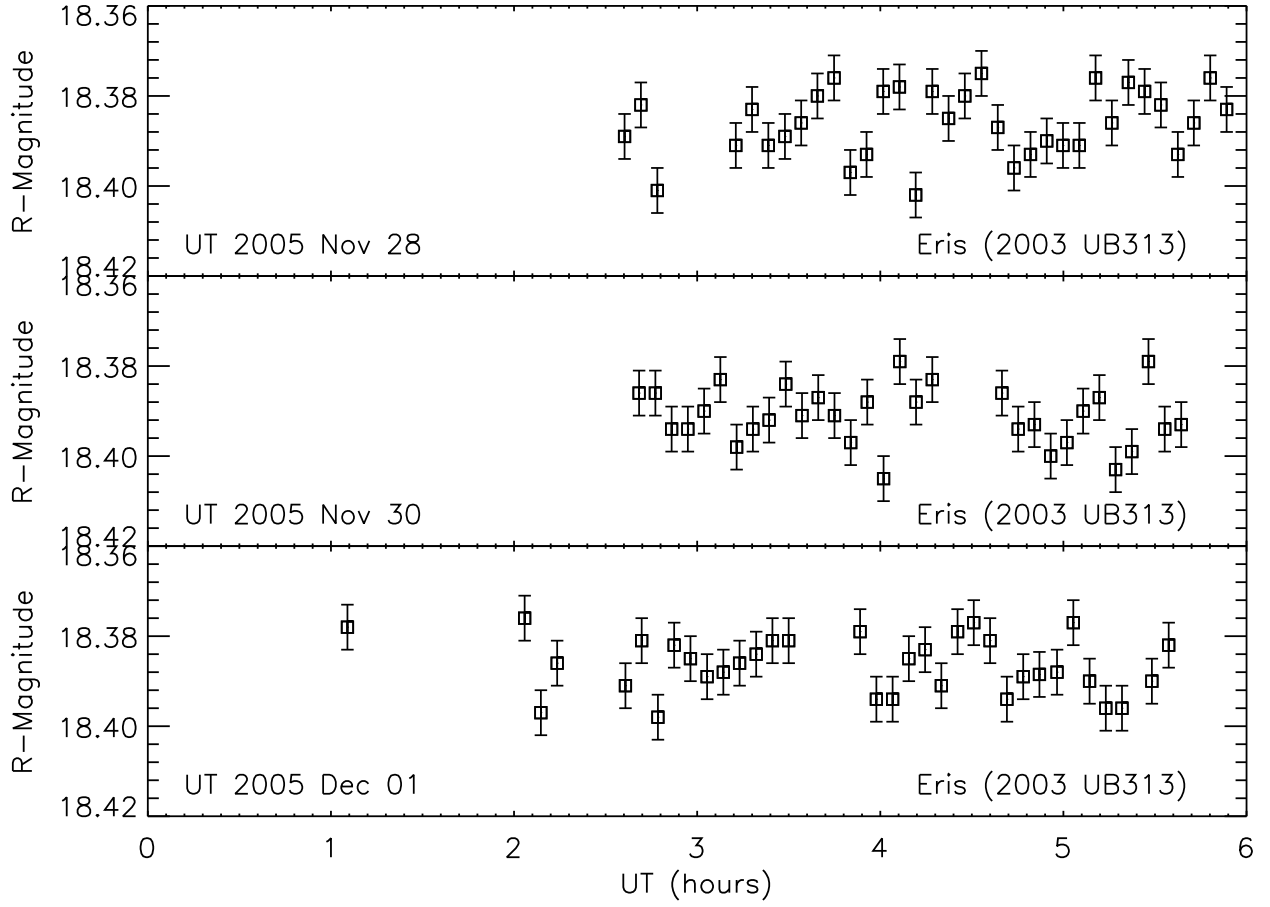


Fig. 17.— The flat light curve of Eris (2003 UB₃₁₃) in November and December 2005. The KBO has no significant short-term variations larger than 0.01 magnitudes over several days.

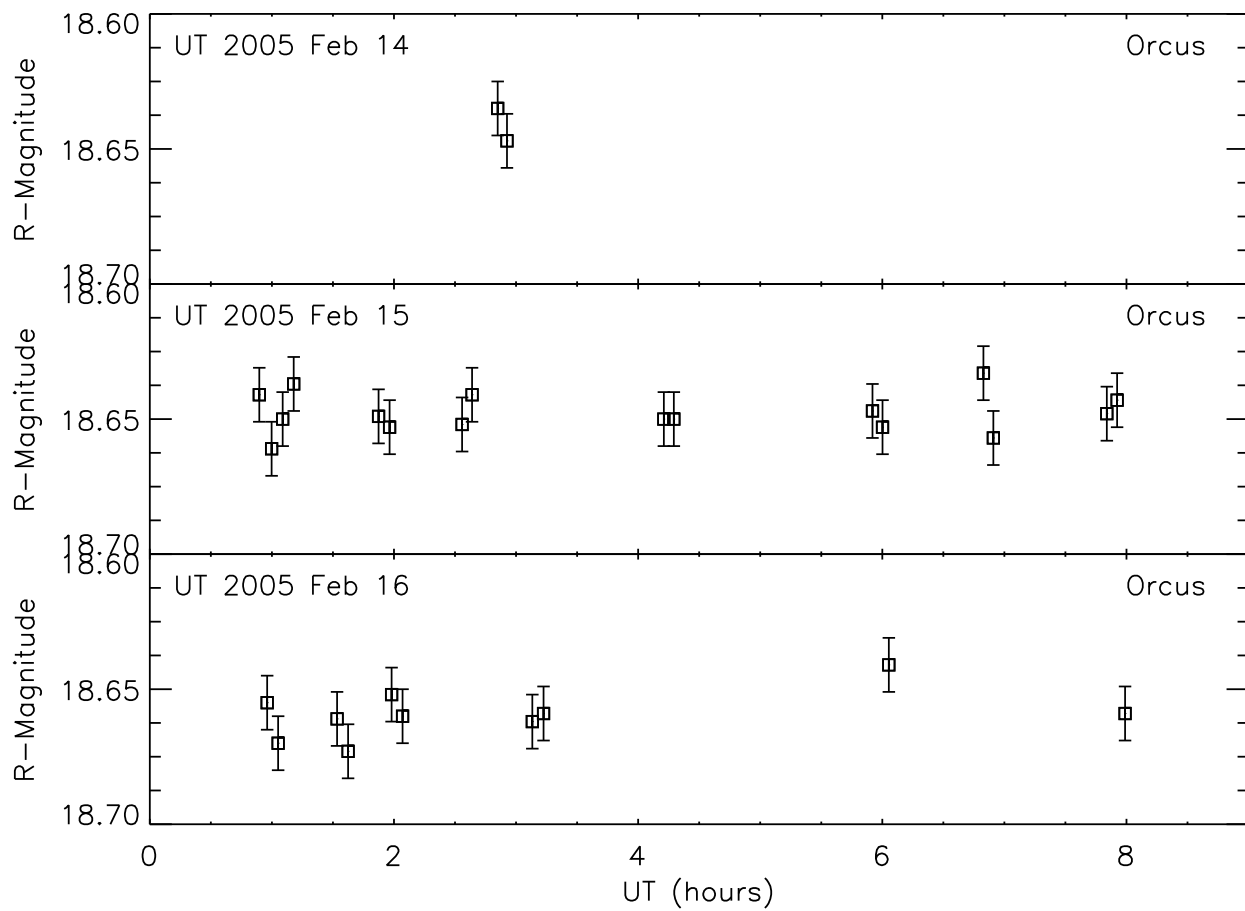


Fig. 18.— The flat light curve of (90482) Orcus 2004 DW in February 2005. The KBO has no significant short-term variations larger than 0.03 magnitudes over several days.

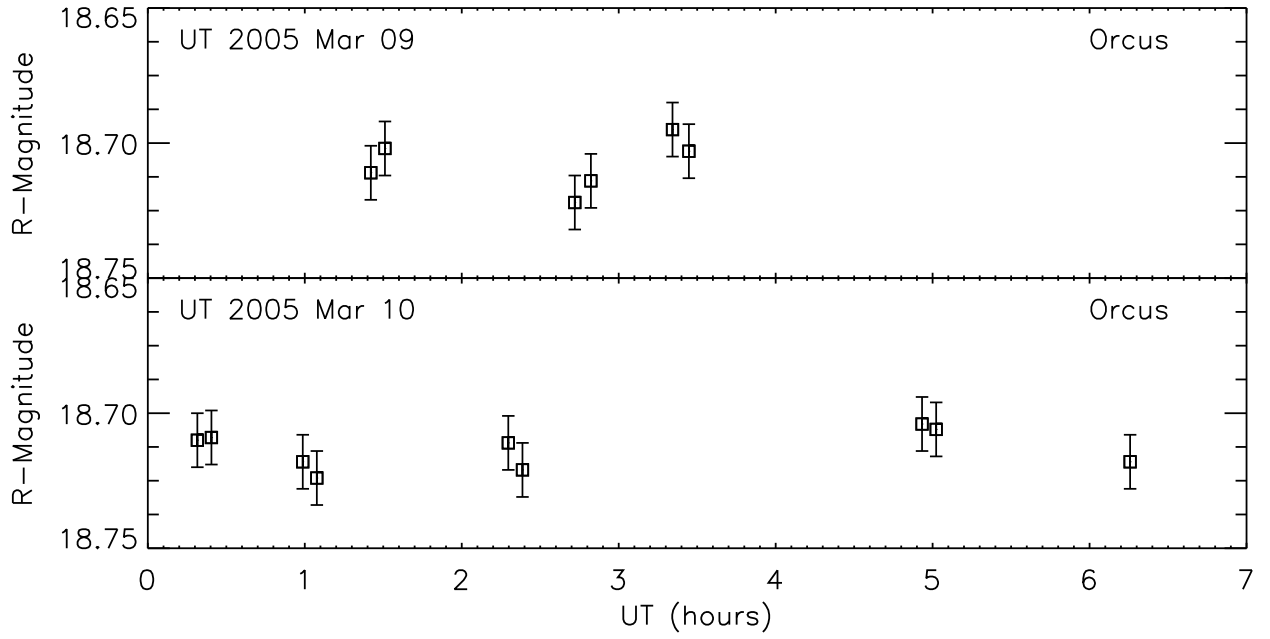


Fig. 19.— The flat light curve of (90482) Orcus 2004 DW in March 2005. The KBO has no significant short-term variations larger than 0.03 magnitudes over several days.

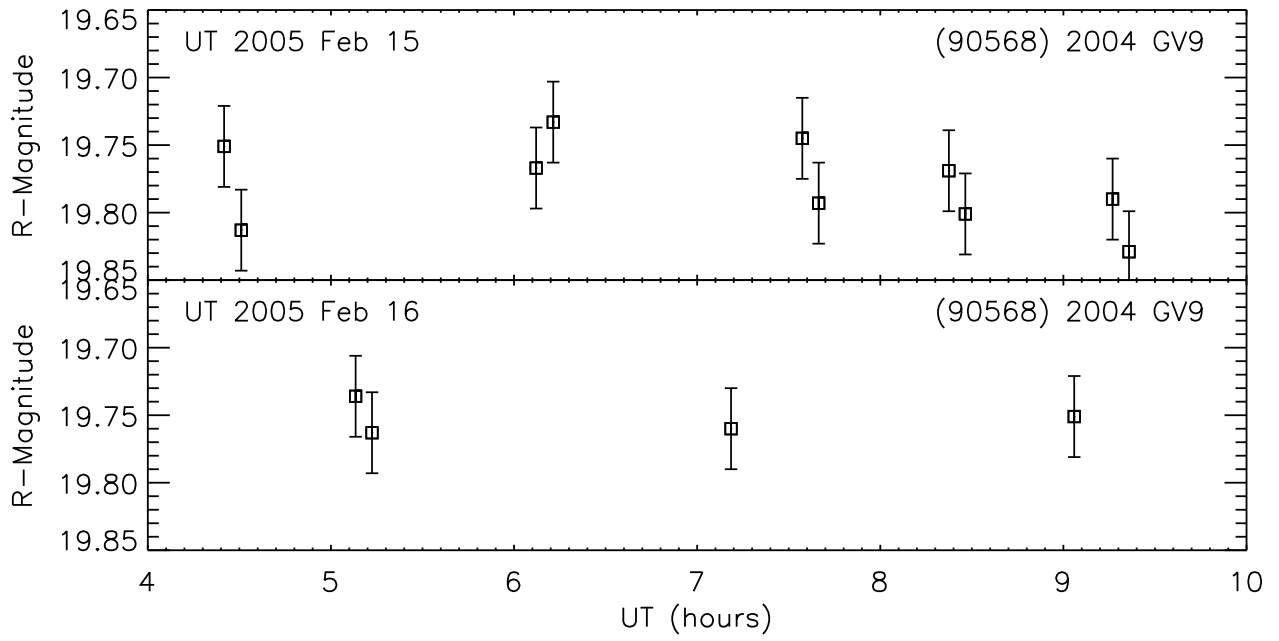


Fig. 20.— The flat light curve of (90568) 2004 GV₉ in February 2005. The KBO has no significant short-term variations larger than 0.1 magnitudes over several days.

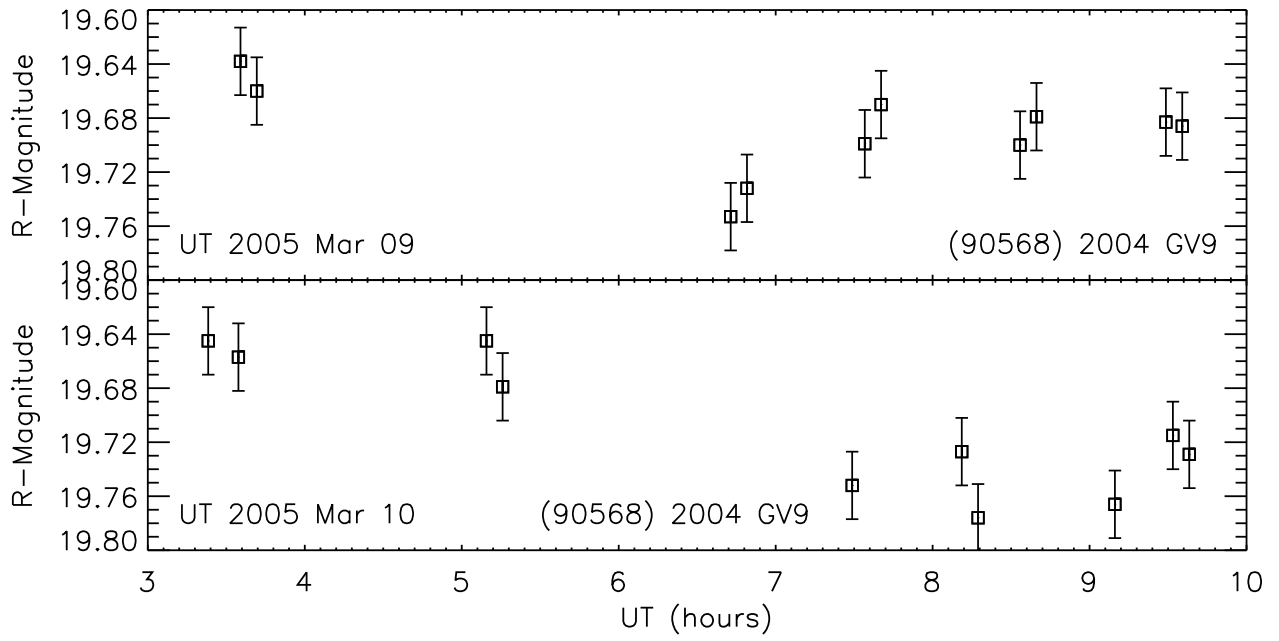


Fig. 21.— The flat light curve of (90568) 2004 GV₉ in March 2005. The KBO has no significant short-term variations larger than 0.1 magnitudes over several days.

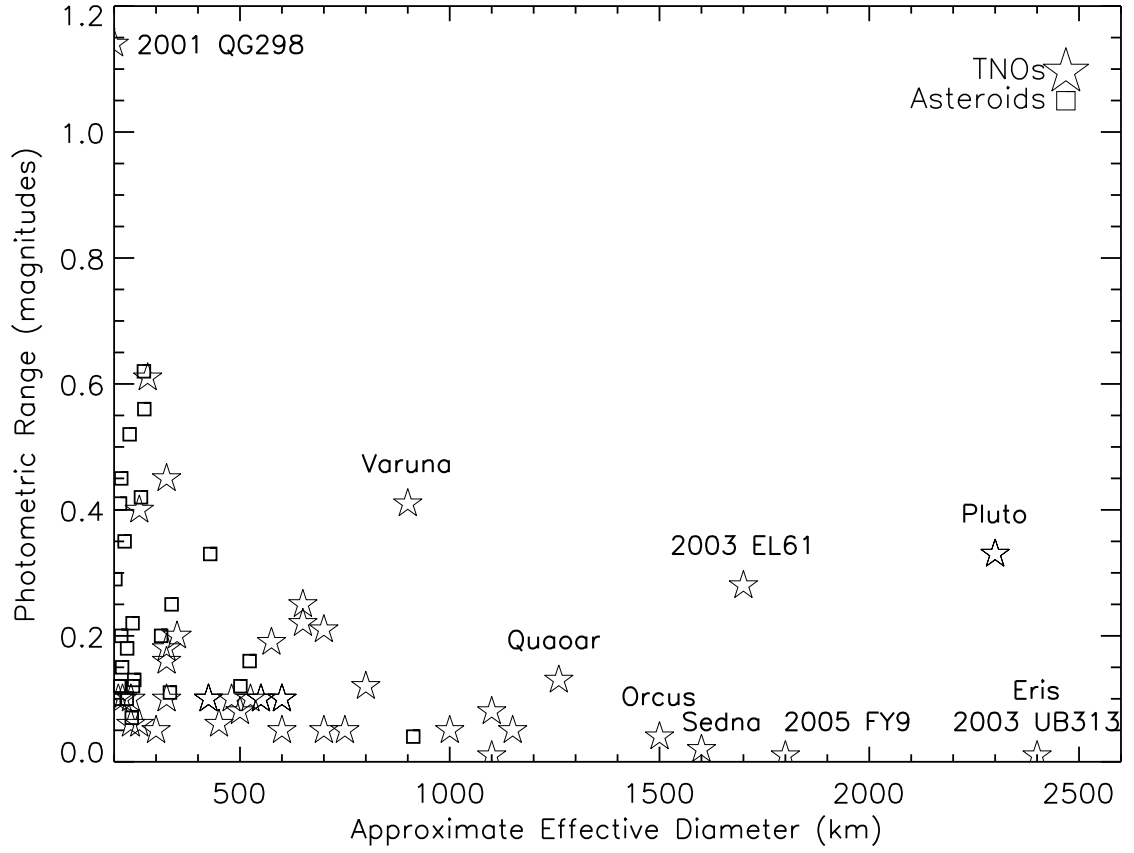


Fig. 22.— This plot shows the diameter of asteroids and TNOs versus their light curve amplitudes. The TNOs sizes if unknown assume they have moderate albedos of about 10 percent. For objects with flat light curves they are plotted at the variation limit found by observations.

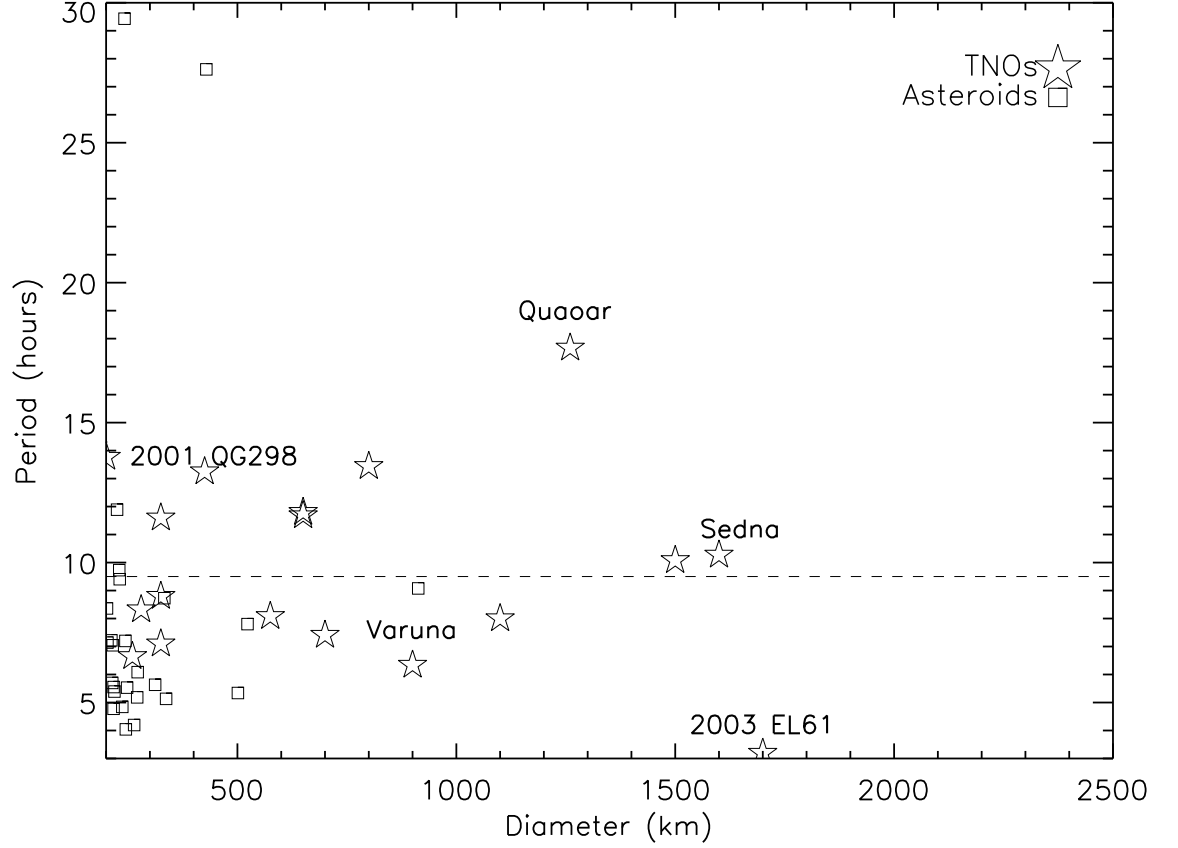


Fig. 23.— Same as the previous figure except the diameter versus the light curve period is plotted. The dashed line is the median of known TNOs rotation periods (9.5 ± 1 hours) which is significantly above the median large MBAs rotation periods (7.0 ± 1 hours). Pluto falls off the graph in the upper right corner because of its slow rotation created by the tidal locking to its satellite Charon.

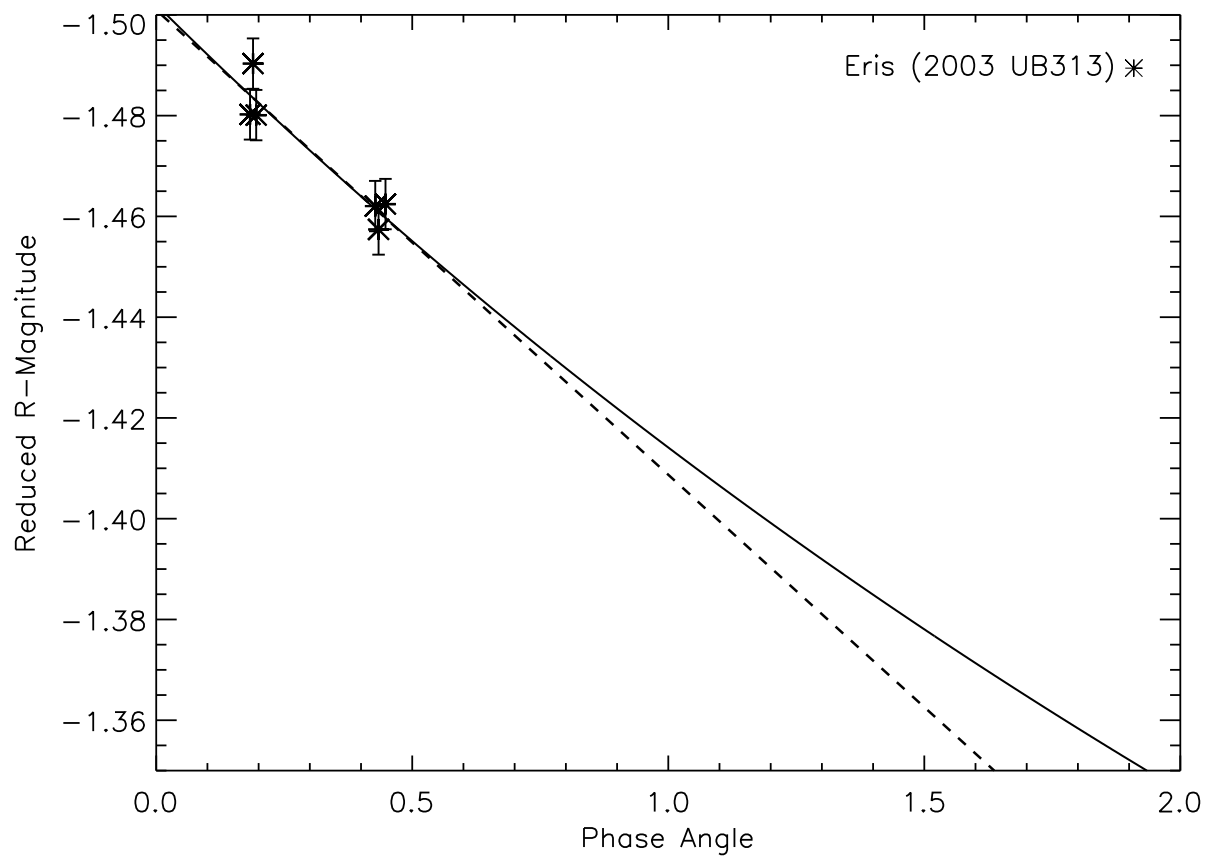


Fig. 24.— The phase curve for Eris (2003 UB₃₁₃). The dashed line is the linear fit to the data while the solid line uses the *Bowell et al. (1989)* H-G scattering formalism. In order to create only a few points with small error bars, the data has been averaged for each observing night.

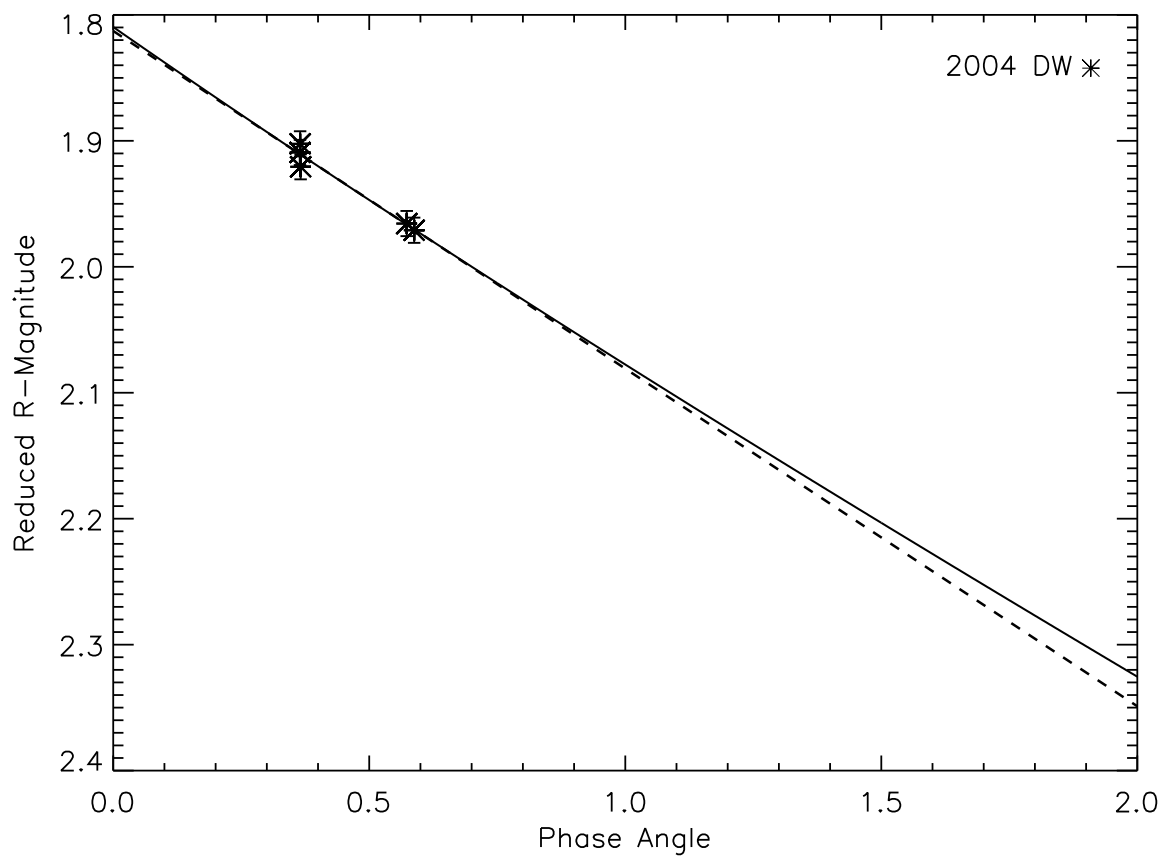


Fig. 25.— The phase curve for (90482) Orcus 2004 DW. The dashed line is the linear fit to the data while the solid line uses the Bowell et al. (1989) H-G scattering formalism. In order to create only a few points with small error bars, the data has been averaged for each observing night.

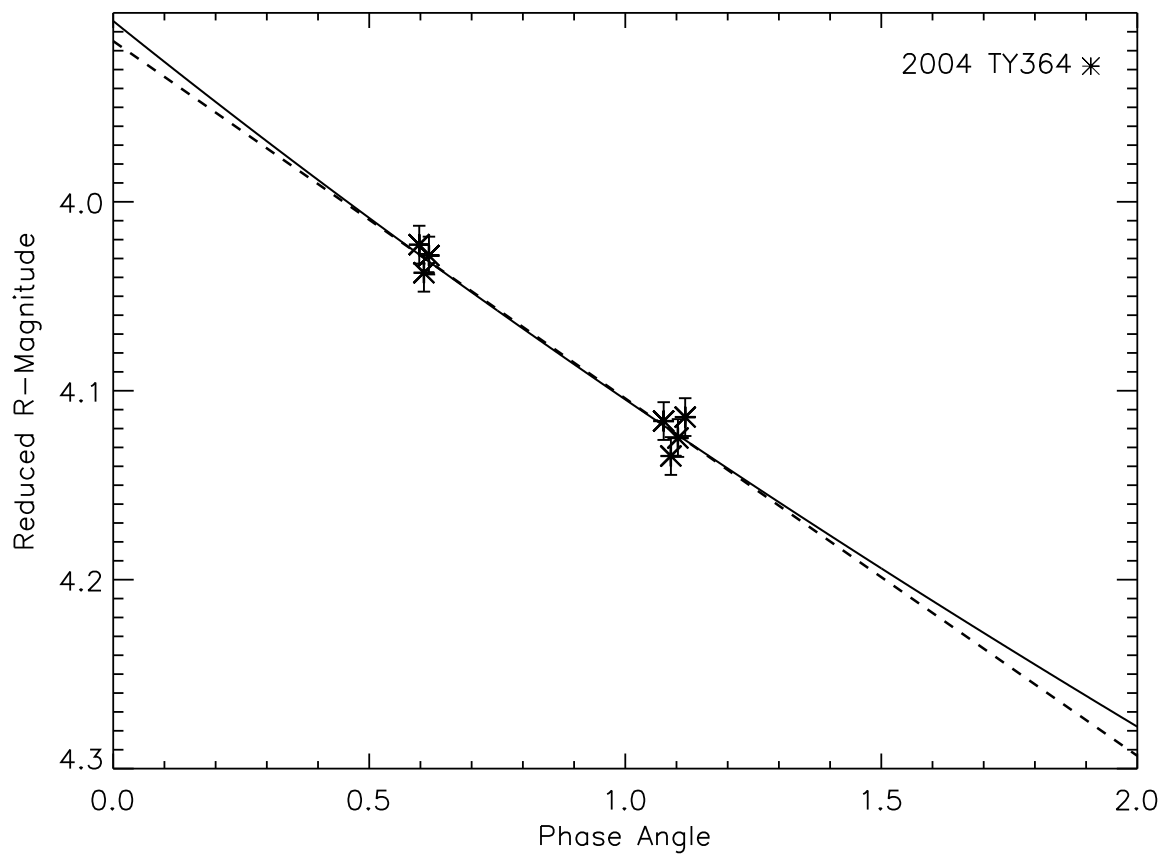


Fig. 26.— The phase curve for (120348) 2004 TY₃₆₄. The dashed line is the linear fit to the data while the solid line uses the *Bowell et al. (1989)* H-G scattering formalism. In order to create only a few points with small error bars, the data has been averaged for each observing night.

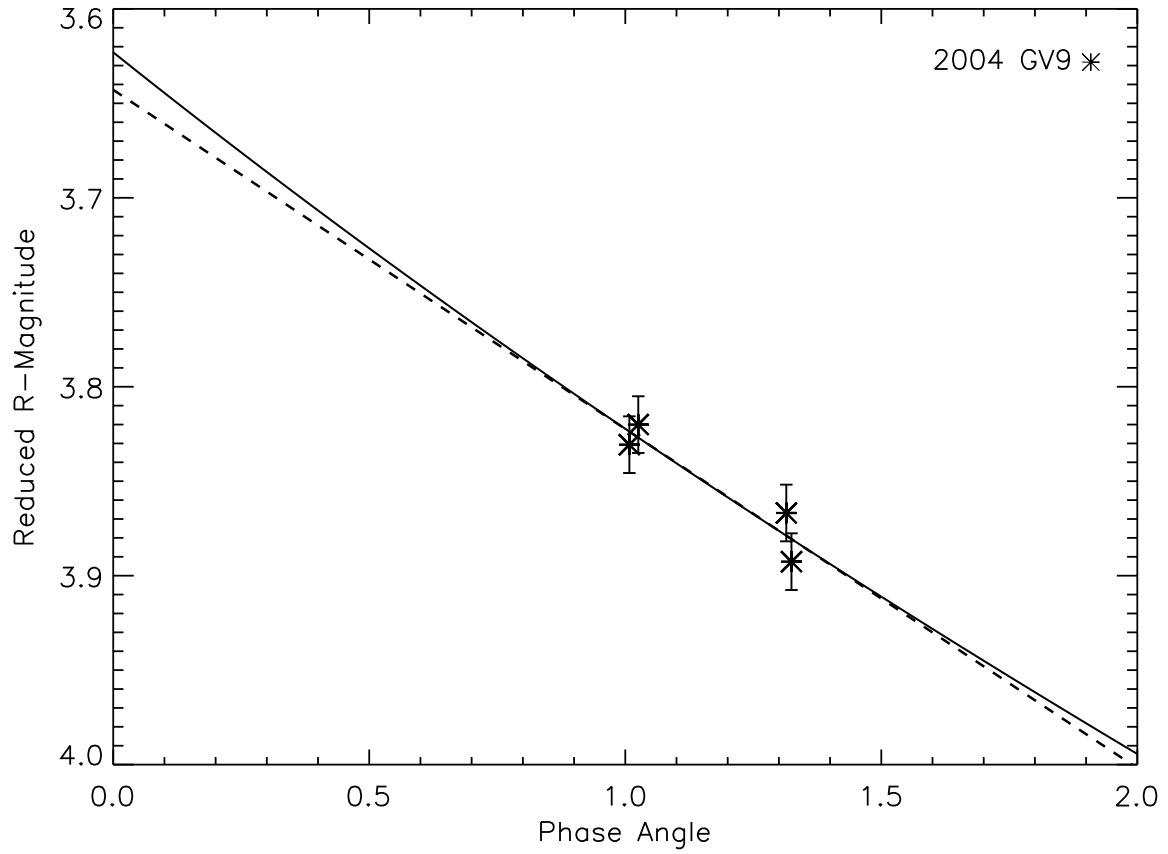


Fig. 27.— The phase curve for (90568) 2004 GV₉. The dashed line is the linear fit to the data while the solid line uses the *Bowell et al. (1989)* H-G scattering formalism. In order to create only a few points with small error bars, the data has been averaged for each observing night.

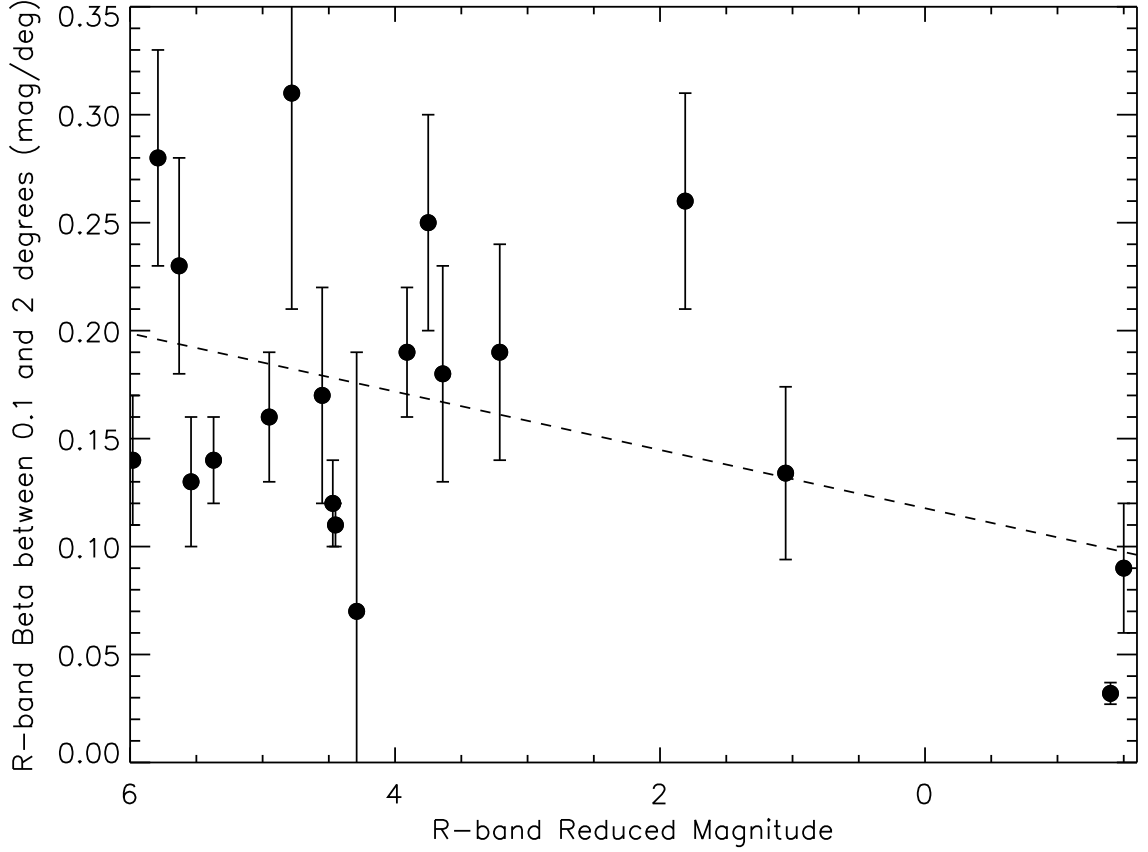


Fig. 28.— The R-band reduced magnitude versus the R-band linear phase coefficient β ($\alpha < 2$ degrees) for TNOs. R-band data is from this work and Sheppard and Jewitt (2002),(2003) as well as Sedna from Rabinowitz et al. (2007) and Pluto from Buratti et al. (2003). A linear fit is shown by the dashed line. Larger objects (smaller reduced magnitudes) may have smaller β at the 97% confidence level using the Pearson correlation coefficient.

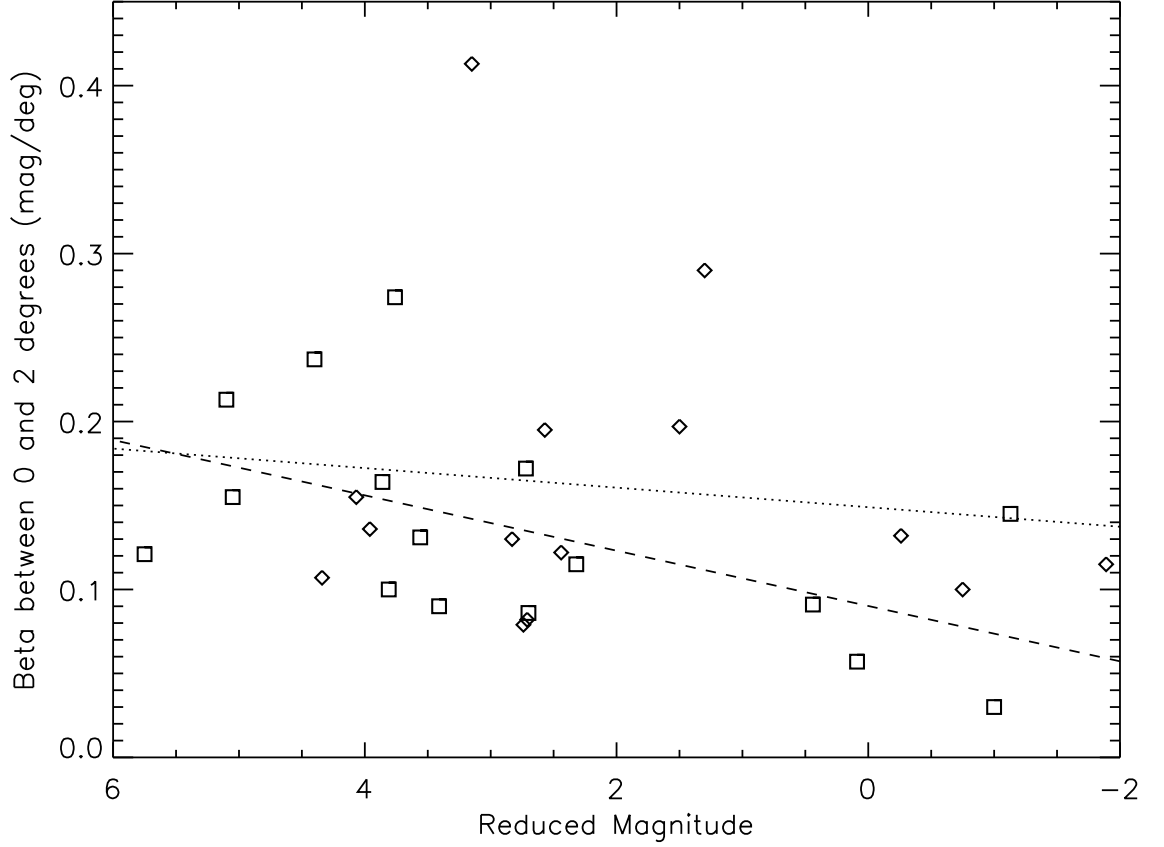


Fig. 29.— Same as Figure 28 except for the V-band (squares) and I-band (diamonds). Pluto and Charon data are from Buie et al. (1997) and the other data are from Rabinowitz et al. (2007). Error bars are usually less than 0.04 mags/deg. The V-band data shows a similar correlation (97% confidence, dashed line) as found for the R-band data in Figure 28, that is larger objects may have smaller β . There is no correlation found using the I-band data (dotted line).

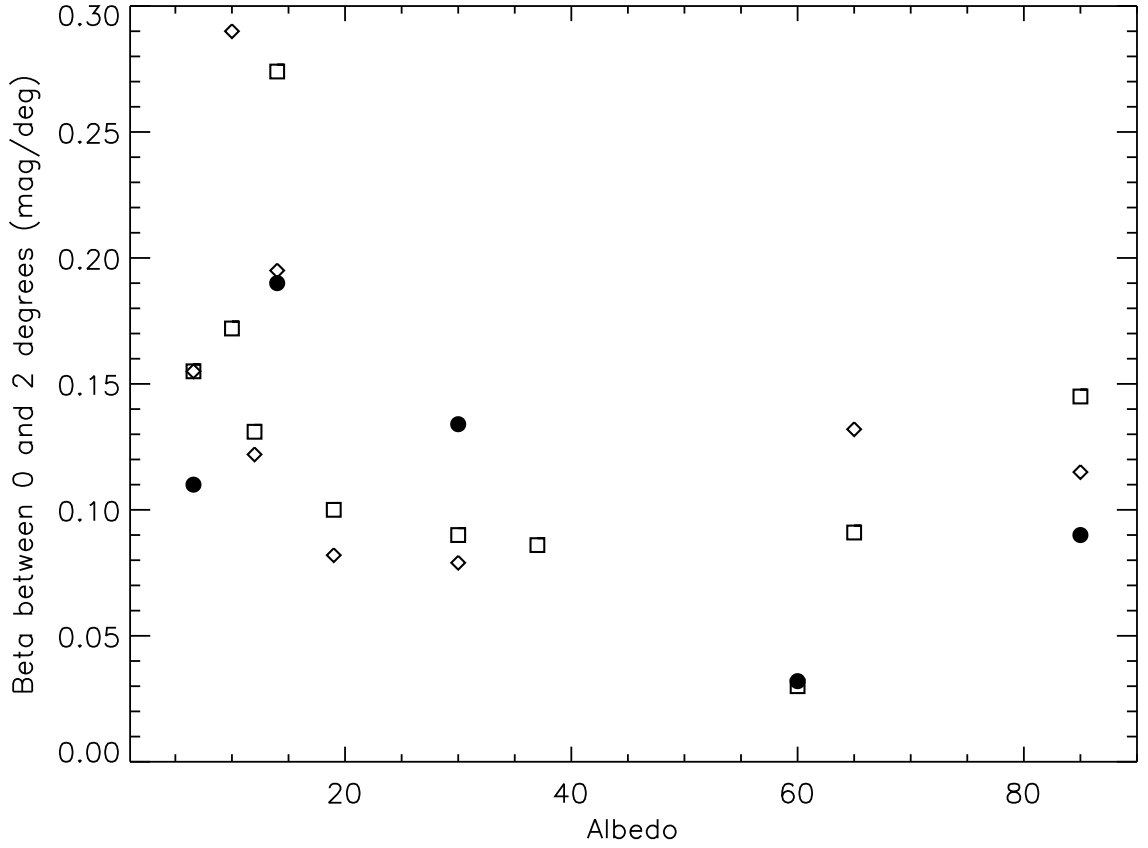


Fig. 30.— Same as Figures 28 and 29 except is the albedo versus linear phase coefficient for TNOs. Filled circles are R-band data, squares are V-band and diamonds are I-band data. Albedos are from Cruikshank et al. (2006).

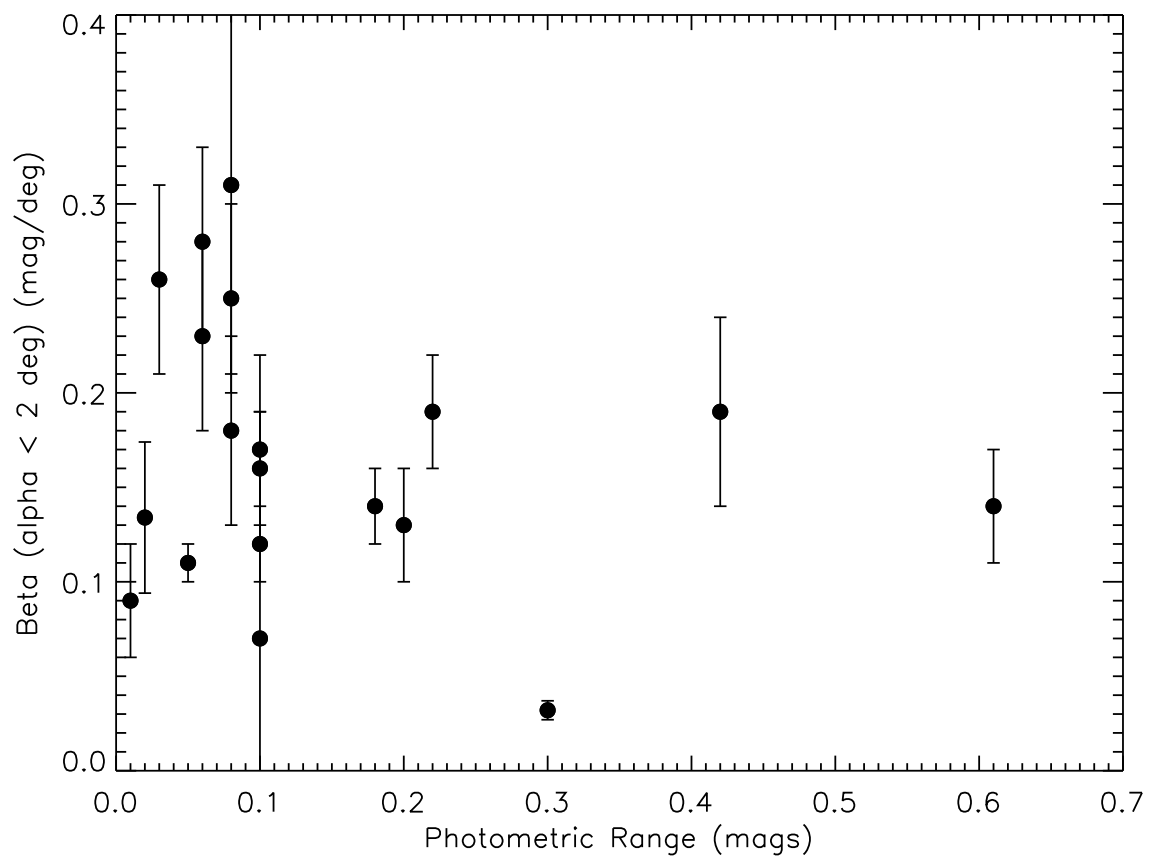


Fig. 31.— Same as Figure 28 except is the light curve amplitude versus the linear phase coefficient for TNOs. TNOs with no measured rotational variability are plotted with their possible amplitude upper limits. No significant correlation is found.

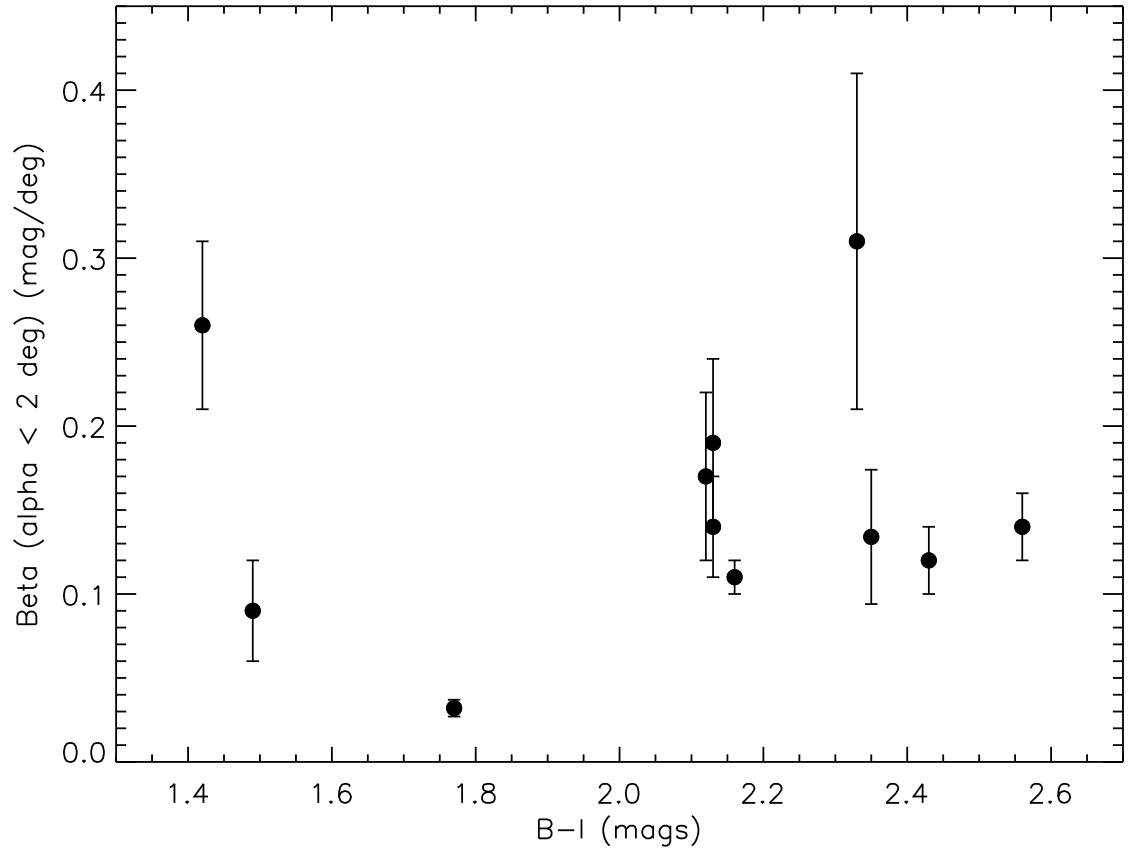


Fig. 32.— Same as Figure 28 except is the B-I broad band colors versus the linear phase coefficient for TNOs. Colors are from Barucci et al. (2005). No significant correlation is found.